Australian Government | ANSTO

Infrared Microspectroscopy (IRM) Beamline

Overview and recent highlights on beamline capabilities

Jitraporn (Pimm) Vongsvivut

Senior Scientist – IRM Beamline

ANSTO – Australian Synchrotron

jitrapov@ansto.gov.au

Science. Ingenuity. Sustainability.

OVERVIEW

- **Traditional Sampling Methods**
  - *Transmission* with 4-angle polarisation analysis
  - *Reflectance* for *in-situ* monitoring of chemical and catalysis reactions

- **Macro-ATR Technique and Recent Applications***
  - Novel *Spirulina* bioactive wound healing coating
  - New *β-carotene* microcapsules using plant protein complexes

- **Progress on New Piezo-Controlled ATR Technique****
  - *In-situ* monitoring of electrochemical reaction in batteries

***Ref:** **J. Vongsvivut**, D. Perez-Guaita, B.R. Wood, P. Heraud, K. Khambatta, D. Hartnell, M. Hackett, **M.J. Tobin**, "Synchrotron macro ATR-FTIR microspectroscopy for high-resolution chemical mapping of single cells," *Analyst* (2019) **144**, 3226-3238.

****Ref:** **S. Liu**, **J. Vongsvivut**, Y. Wang, R. Zhang, F. Yang, S. Zhang, K. Davey, J. Mao, and Z. Guo, "Monolithic Phosphate Interphase for Highly Reversible and Stable Zn Metal Anode," *Angew. Chem. Int. Ed.* (2023), **62**, *4*, e202215600.

TRADITIONAL SAMPLING METHODS

– *Transmission* with 4-Angle Polarisation Analysis –

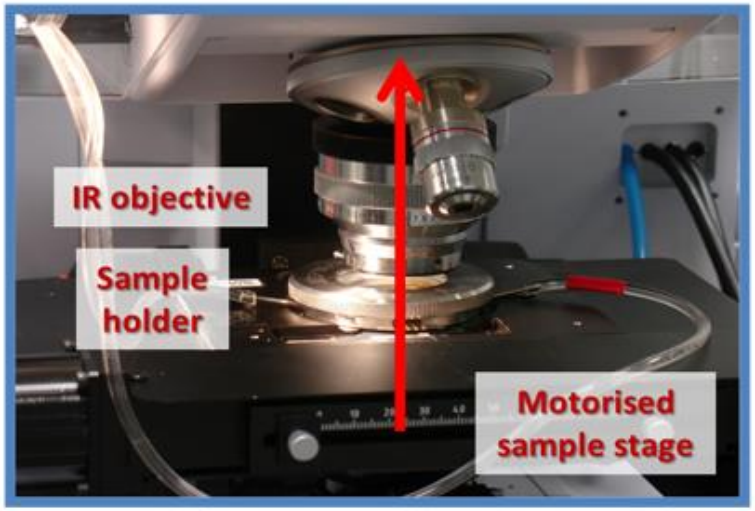

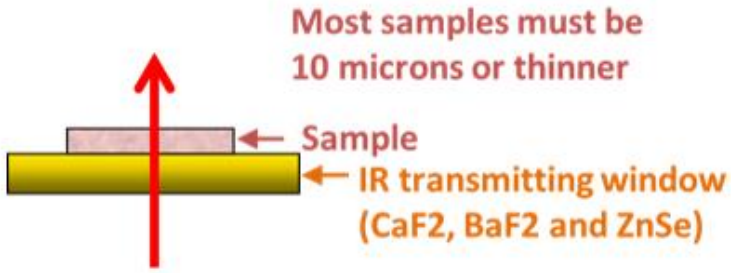

ANSTO

POLARISED-IR SPECTROSCOPY

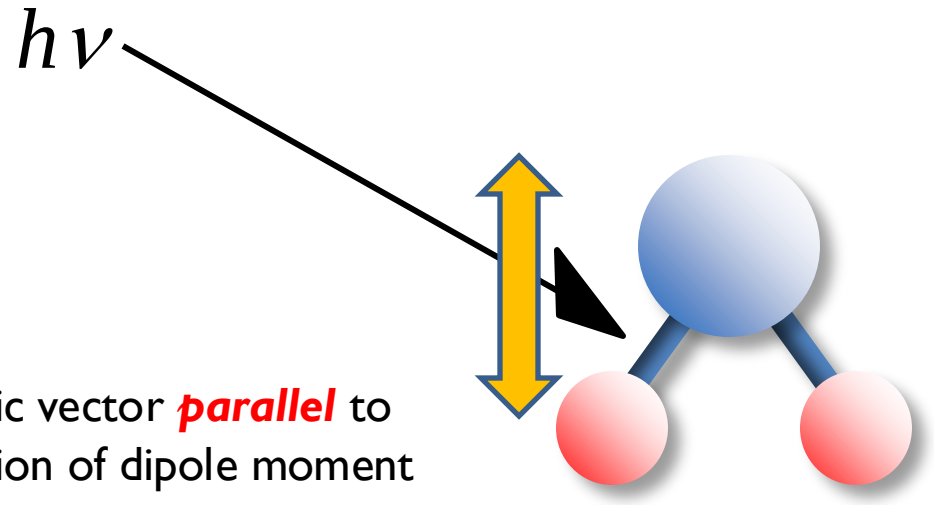

Electric vector ***parallel*** to direction of dipole moment change

STRONG ABSORBANCE

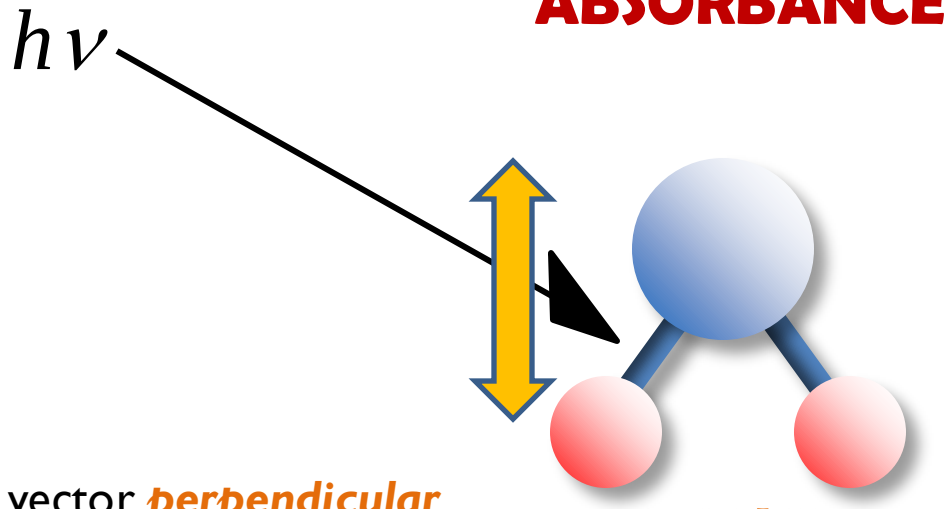

Electric vector ***perpendicular*** to direction of dipole moment change

WEAK ABSORBANCE

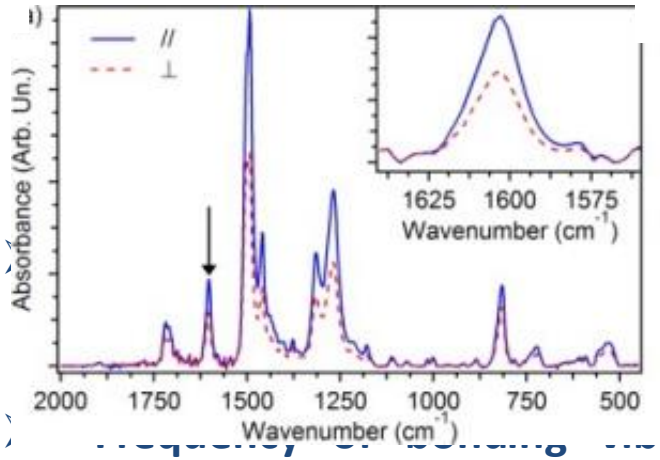

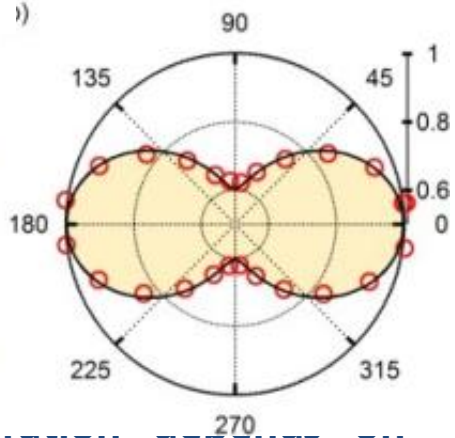

- **Frequency of bonding vibration depends on mass of atoms and strength of bond.**

Reference: V. Fasano, A. Polini, G. Morello, M. Moffa, A. Camposeo, D. Pisignano, *Macromolecules* (2013), **46 (15)**, 5935–5942.

- **Frequency is influenced by surrounding bonds and atoms.**

Absorbance of oriented electrospun polymer fibres

- *Ring stretching mode of the fluorene unit, associated with vibrations prevalently directed along the molecular chain axis*

- **For IR absorption to occur, vibration must result in a net change in dipole moment.**

✓ **Polarised-IR spectroscopy can therefore be used to probe the orientation of molecular bonds and functional groups ☺**

ANSTO

FOUR–ANGLE POLARISATION IR MICROSPECTROSCOPY*

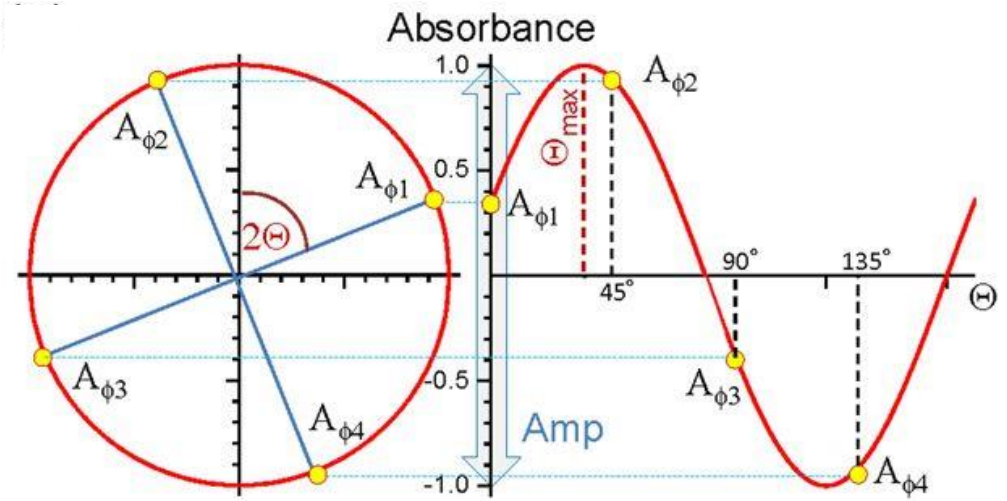

$$f_\psi = \frac{D-1}{D+2} \cdot \frac{2}{3\cos^2\alpha - 1}$$

This is the "orientation function"
a measure of how strongly oriented
the dipole is

Where: $D = \frac{\gamma - \sqrt{a^2+b^2}}{\gamma + \sqrt{a^2+b^2}}$ $\quad a = A_0 - A_{90}$ $\quad b = A_{45} - A_{-45}$

$$Amp = \sqrt{(A_{\phi_4} - A_{\phi_2})^2 + (A_{\phi_3} - A_{\phi_1})^2},$$

$$\theta = \frac{1}{2}\tan^{-1}\left(\frac{A_{\phi_3} - A_{\phi_1}}{A_{\phi_4} - A_{\phi_2}}\right),$$

This is the angle of the vibrating dipole

***Ref:** Y. Hikima, J. Morikawa, T. Hashimoto, "FT-IR image processing algorithms for in-plane orientation function and azimuth angle of uniaxially drawn polyethylene composite film," *Macromolecules* (2011), **44**, 3950–3957.

ANSTO

FOUR–ANGLE POLARISATION IR MICROSPECTROSCOPY

By coupling an FTIR spectrometer to an IR microscope, high quality (signal-to-noise) spectral data can be collected from microscopic samples.

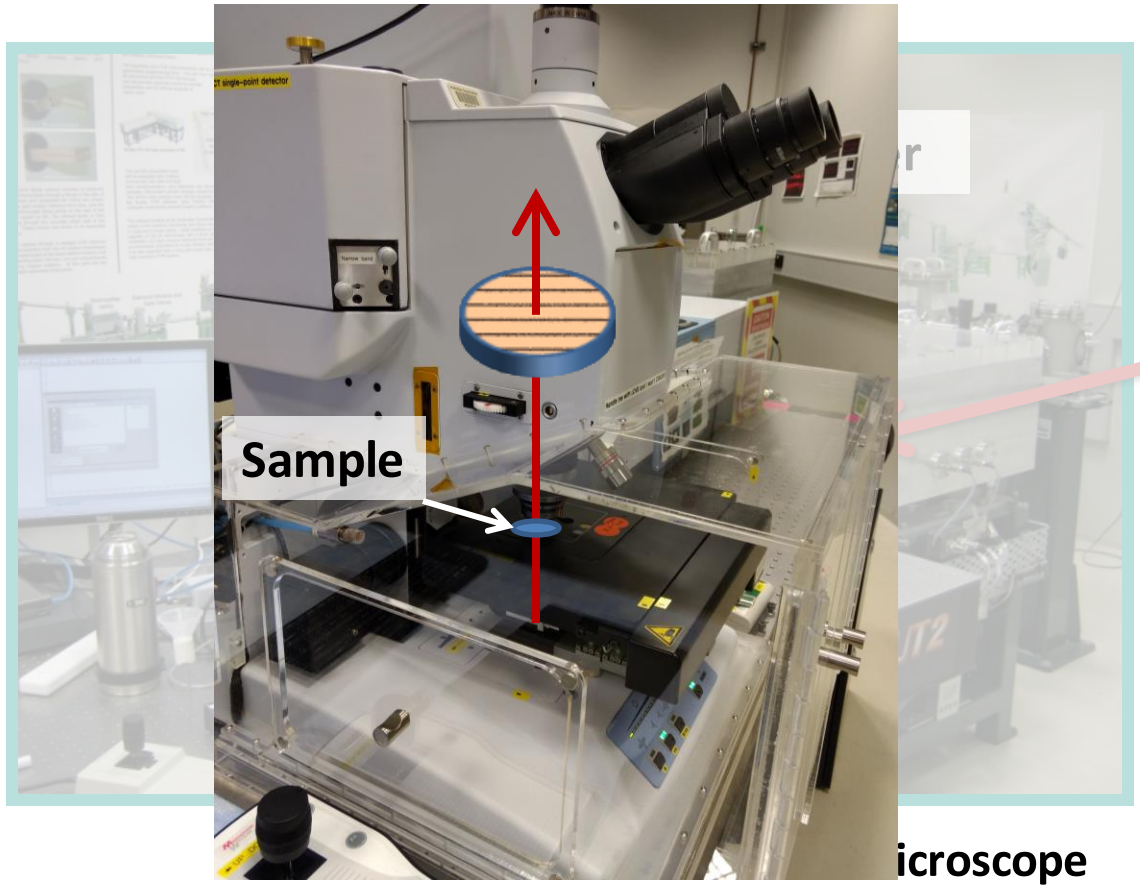

icroscope

Synchrotron Beam

- Synchrotron-IR source and single-point MCT & FPA imaging detectors
- High spatial resolution down to 6-8 μm for transmission and reflectance
- Mid-IR range with MCT (3850-1000 cm^{-1})
- Mid-/Far-IR range with Si:B photodetector (6000-380 cm^{-1})

TRANSMISSION ❶

Laser modification of silk protein for tissue scaffold printing: orientational hyper-spectral imaging of silk

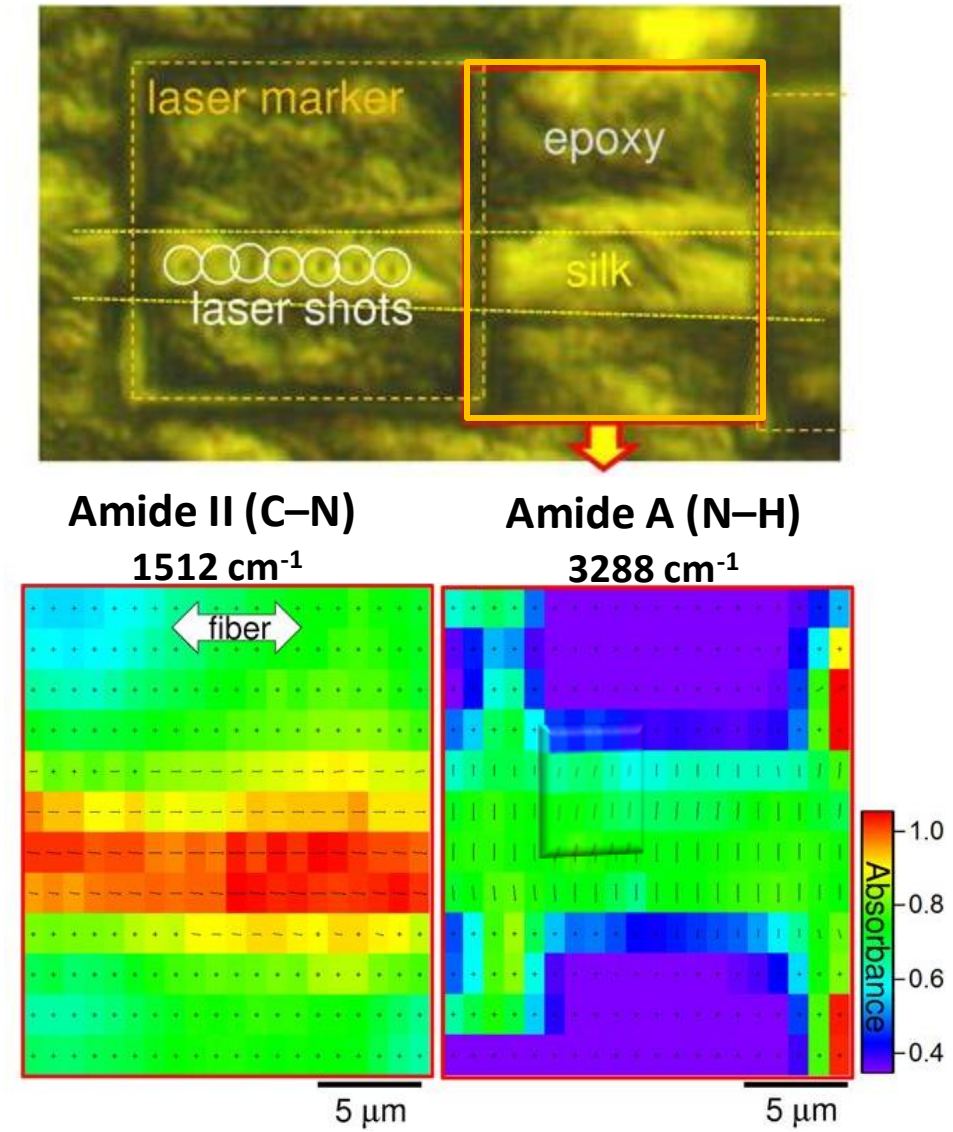

Bar direction = θ
dipole azimuth angle

Bar length = f_ψ
Orientation Function

Ref [1]: M. Ryu *et al*., "Orientational Mapping Augmented Sub-Wavelength Hyper-Spectral Imaging of Silk," *Sci. Rep.* (2017) **7**, 7419.
Ref [2]: M. Ryu *et al*., "Nanoscale Chemical Mapping of Laser-Solubilized Silk," *Mater. Res. Express* (2017) **4 (11)**, 115028.

TRANSMISSION 2

Gain a better understanding the enhanced solubility of paracetamol *form II* through their orientation using polarised IR mapping analysis

SWINBURNE UNIVERSITY OF TECHNOLOGY

Tokyo Institute of Technology

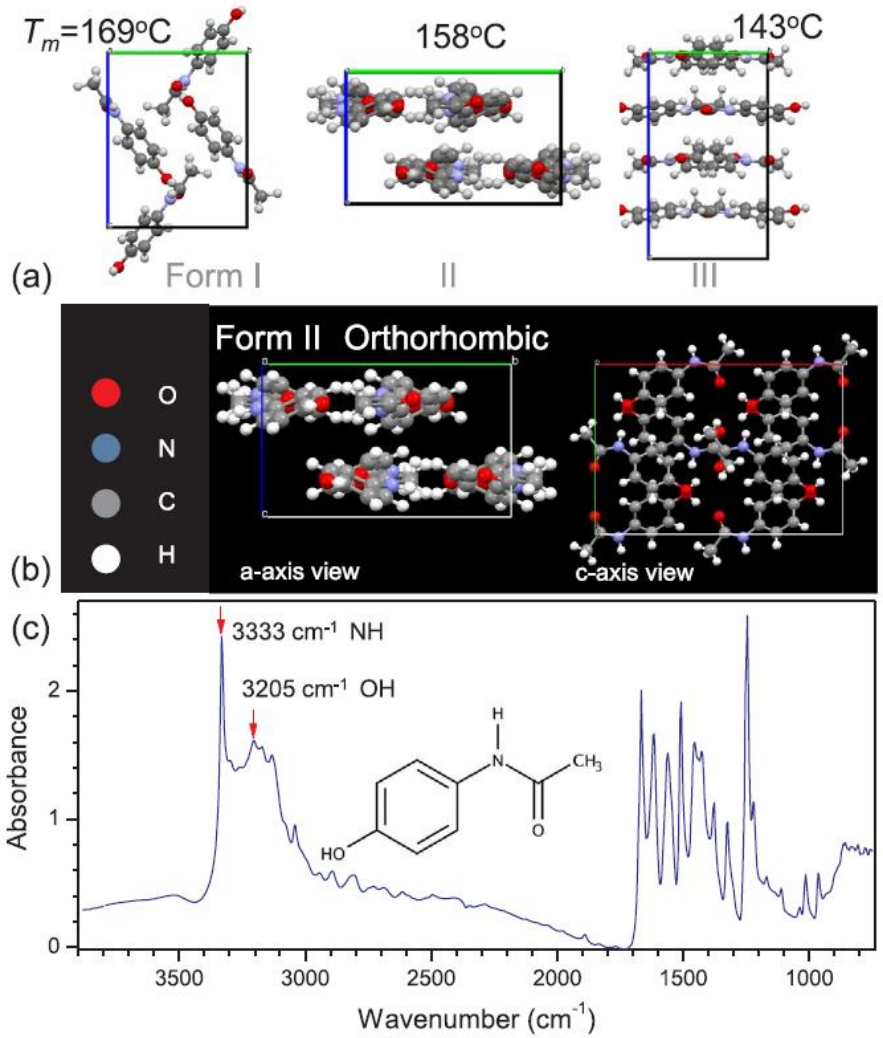

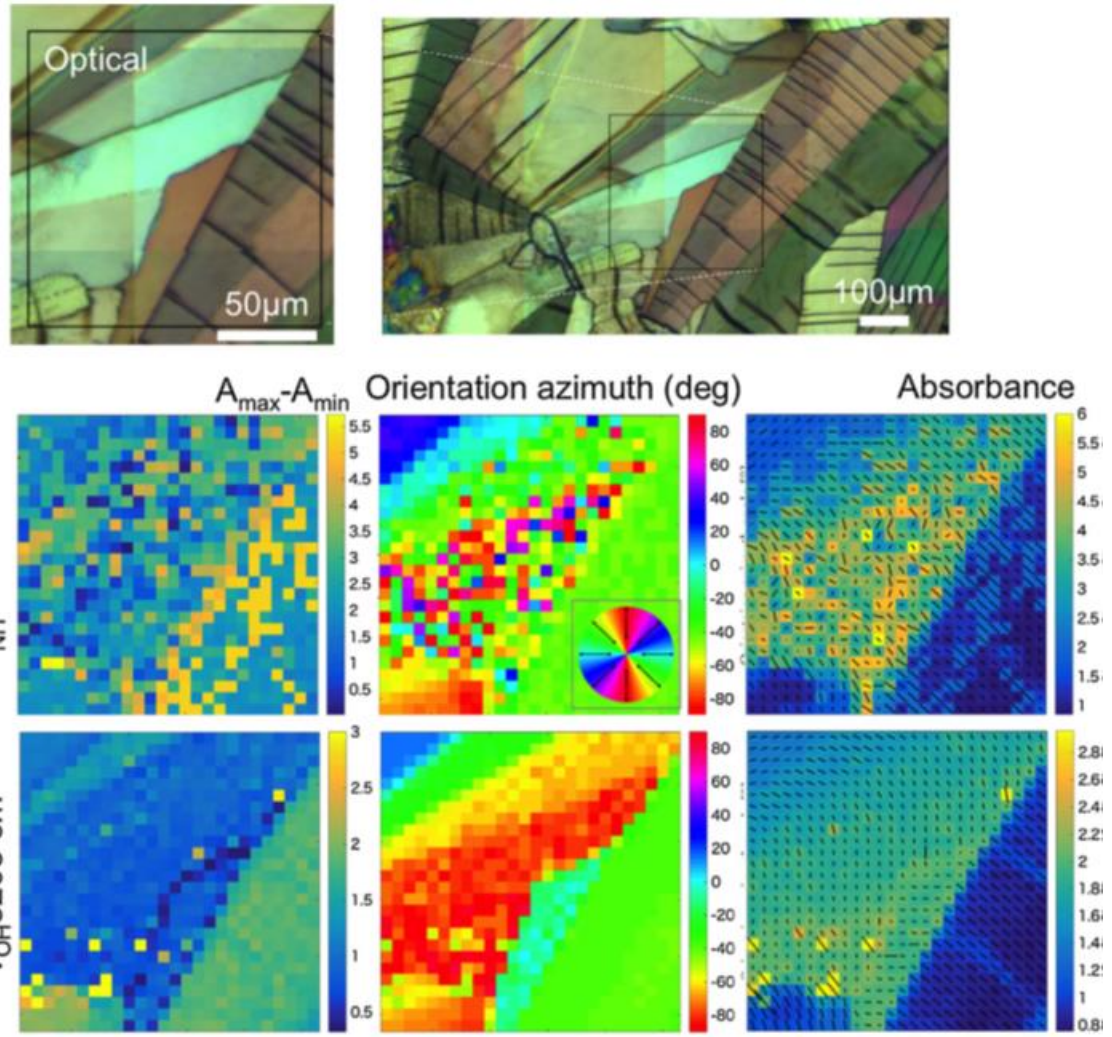

Ref: R. Honda, M. Ryu, A. Balčytis, **J. Vongsvivut**, **M.J. Tobin**, S. Juodkazis, J. Morikawa, "Paracetamol micro-structure analysis by optical mapping," *Appl. Surf. Sci.* (2019), **473**, 127–132.

TRANSMISSION 3

Improving the mechanical performance of PLA by using nano-crystalline cellulose as fillers to produce durable biodegradable composite material

Use of additives such as nanocrystalline starch and cellulose has shown *improved mechanical properties of the PLA*.

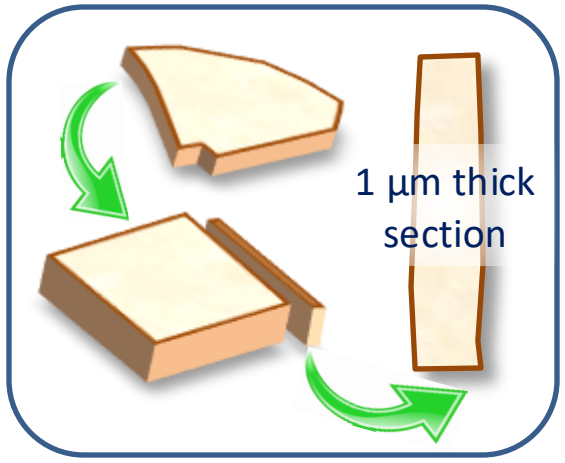

Sample preparation: thin microtomed sections

Transmitted visible light

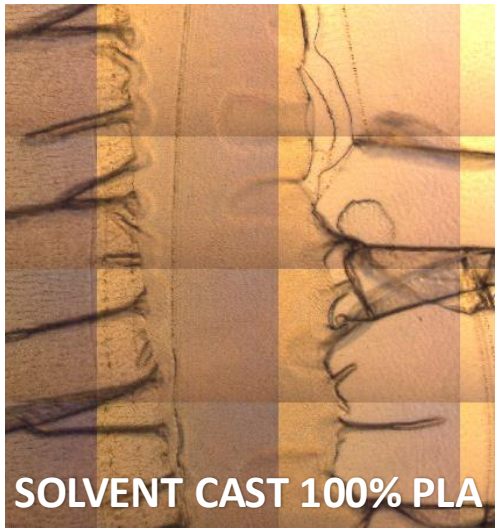

Polarised visible light

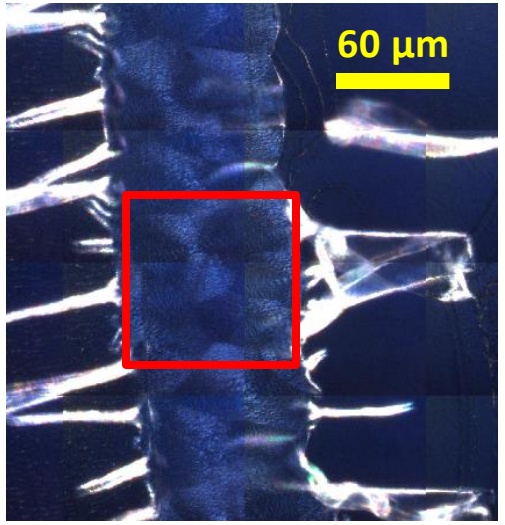

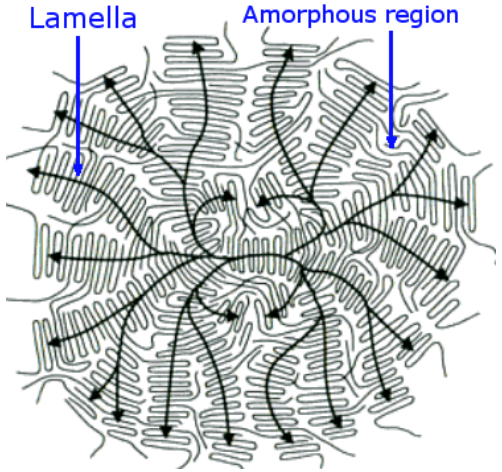

ANSTO

TRANSMISSION 3

Improving the mechanical performance of PLA by using nano-crystalline cellulose as fillers to produce durable biodegradable composite material

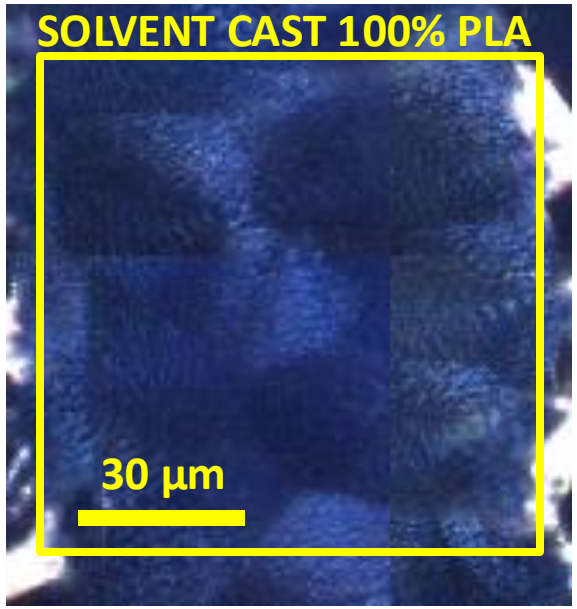

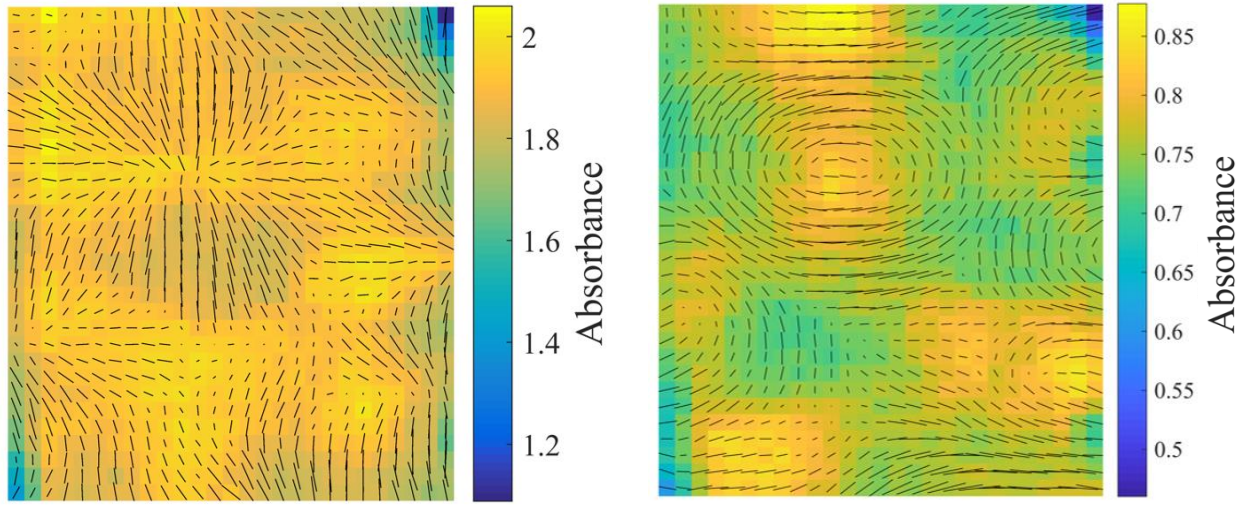

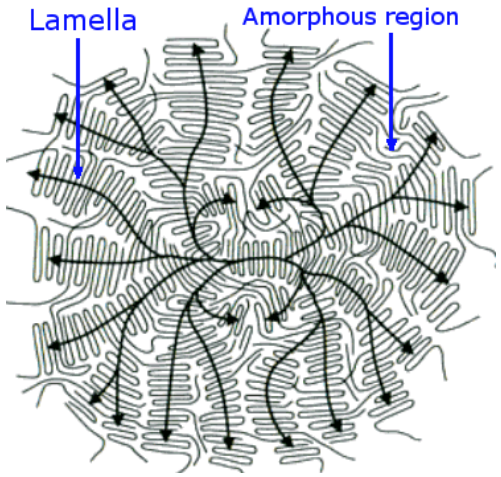

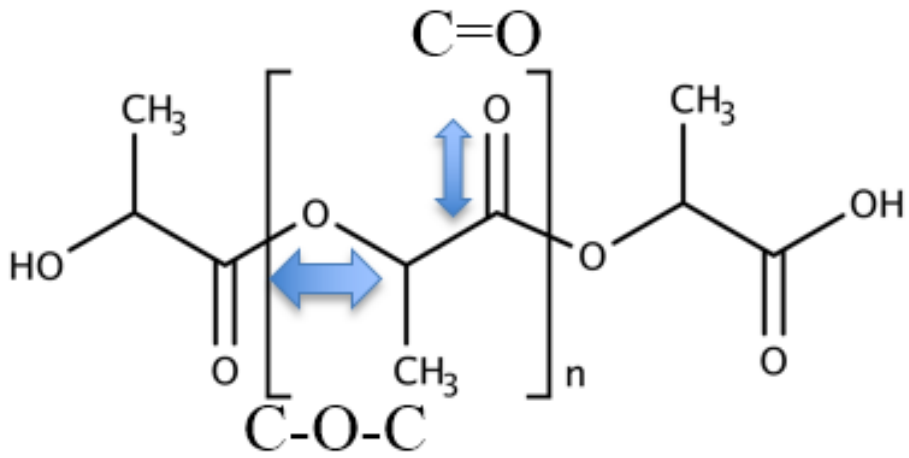

Ref: P. Takkalkar, **M.J. Tobin**, **J. Vongsvivut**, T. Mukherjee, S. Nizamuddin, G. Griffin, N. Kao, "Structural, Thermal, Rheological and Optical Properties of Polylactic Acid Films Prepared Through Solvent Casting and Melt Processing Techniques," *JTICE* (2019), **104**, 293-300.

ANSTO

TRANSMISSION 3

Improving the mechanical performance of PLA by using nano-crystalline cellulose as fillers to produce durable biodegradable composite material

SOLVENT CAST 100% PLA

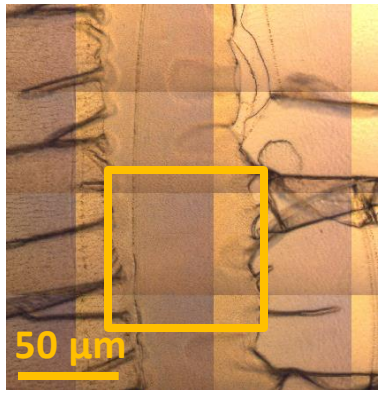

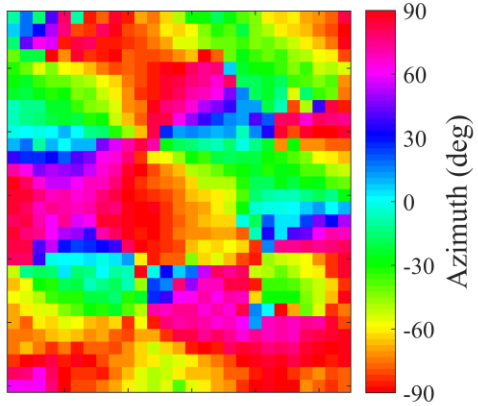

ν(C=O) sidechain

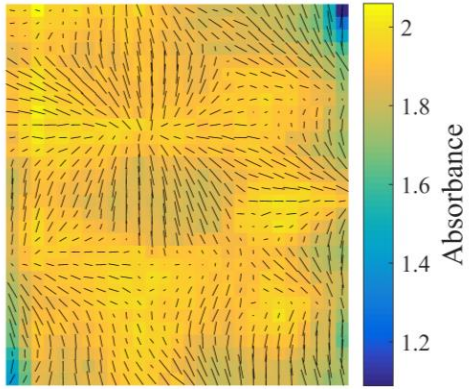

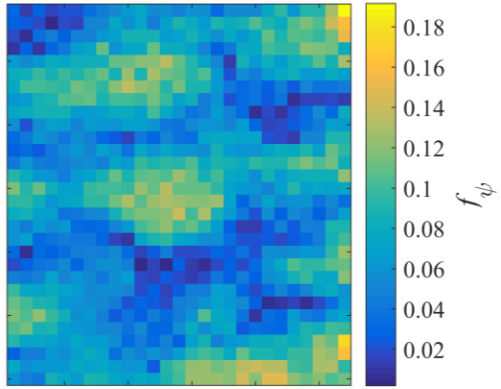

MELT PROCESSED* PLA 5% NANOCRYSTALLINE STARCH

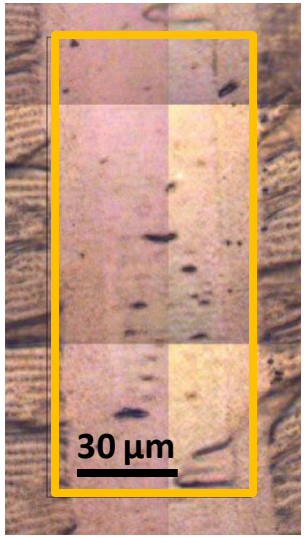

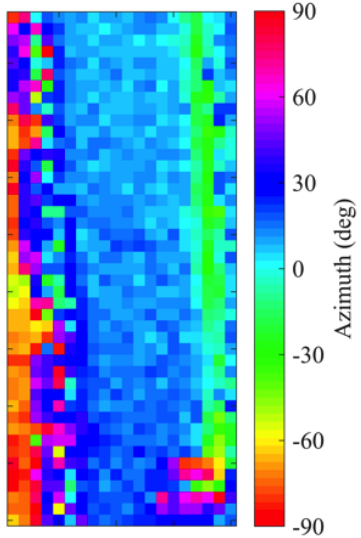

Dipole angle

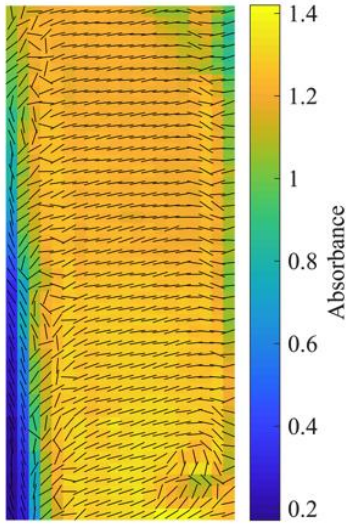

Dipole angle
Orientation Function
Absorbance

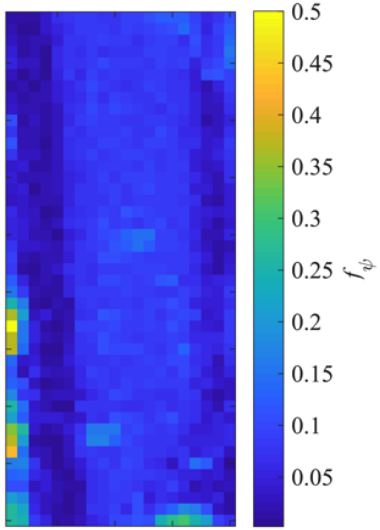

Orientation Function

***MELT PROCESS:**

another way of casting out solvent from polymer.

In this process, the pellet was first heated up, pressed into a dye press and then allowed to cool.

TRANSMISSION 3

Improving the mechanical performance of PLA by using nano-crystalline cellulose as fillers to produce durable biodegradable composite material

SOLVENT CAST 100% PLA

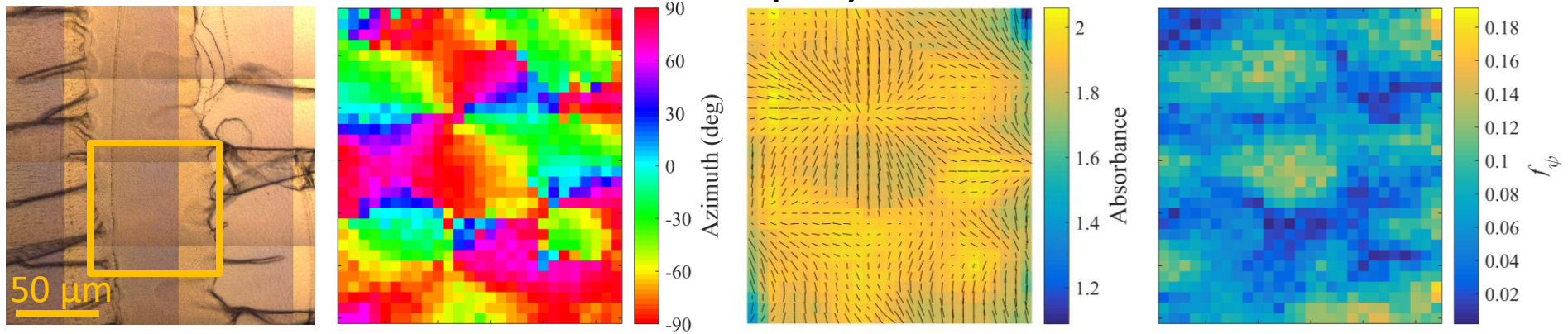

MELT PROCESSED PLA 5% NANOCRYSTALLINE STARCH

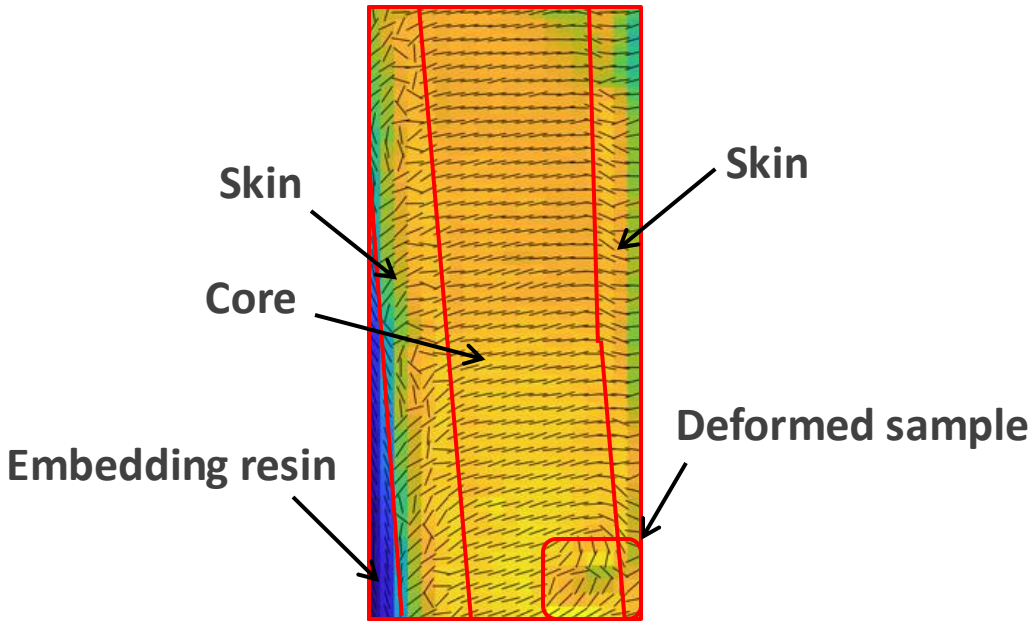

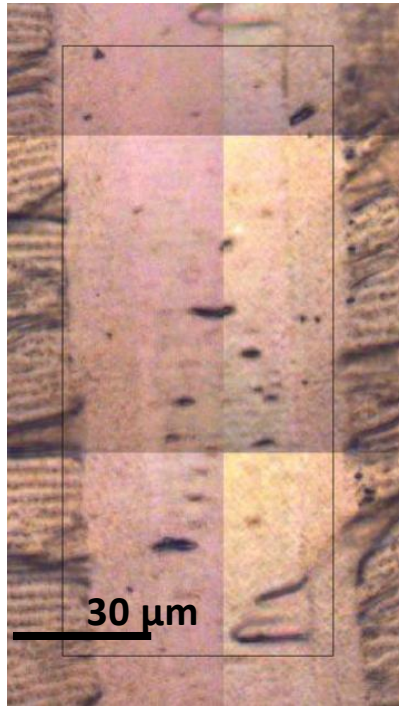

ANSTO

TRANSMISSION 4

Characterization of electrically aligned reduced graphene oxide (rGO) sheets in liquid crystalline elastomer (LCE) used as artificial muscles and soft actuators

SWINBURNE UNIVERSITY OF TECHNOLOGY

Manufacturing Futures Research Institute

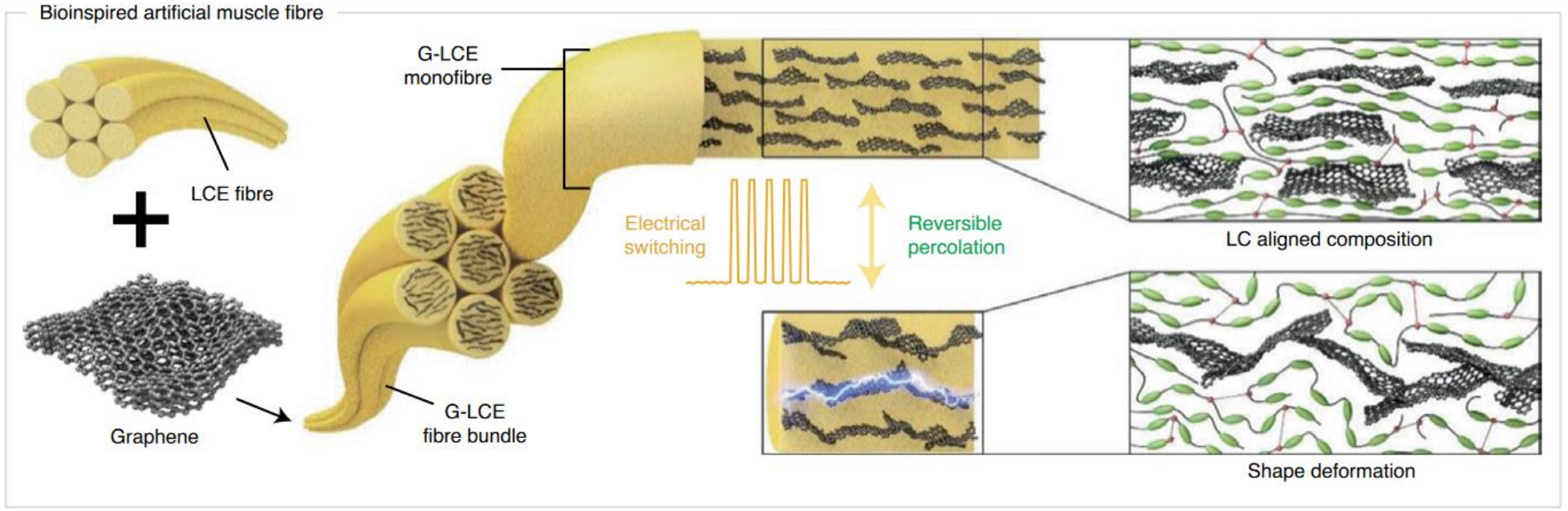

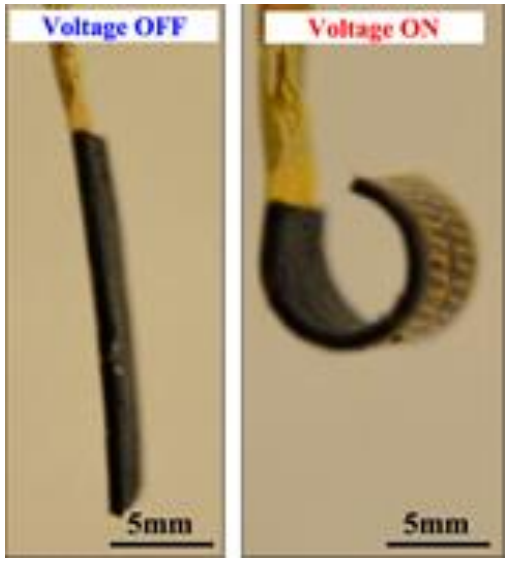

- Using **reduced graphene oxide (rGO)** to enhance the conductivity of thermally responsive LCEs, that have been used as artificial muscles and soft actuators for robotic and sensor applications.
- **This project aims at investigating the effect of applied electrical fields on the alignment of rGO embedded within the matrix of LCE, to gain insights into its structure-property relationship** critical for underpinning the performance enhancement of these artificial muscles.

Ref: J. Ince, A. Al-qatatsheh, **J. Vongsvivut**, S. Juodkazis, N. Hameed, N. Salim, "Characterization of electrically aligned reduced graphene oxide sheets in liquid crystalline elastomer matrices," *manuscript in preparation*.

TRANSMISSION 4

Characterization of electrically aligned reduced graphene oxide (rGO) sheets in liquid crystalline elastomer (LCE) used as artificial muscles and soft actuators

SWINBURNE UNIVERSITY OF TECHNOLOGY

Electrical conductivity

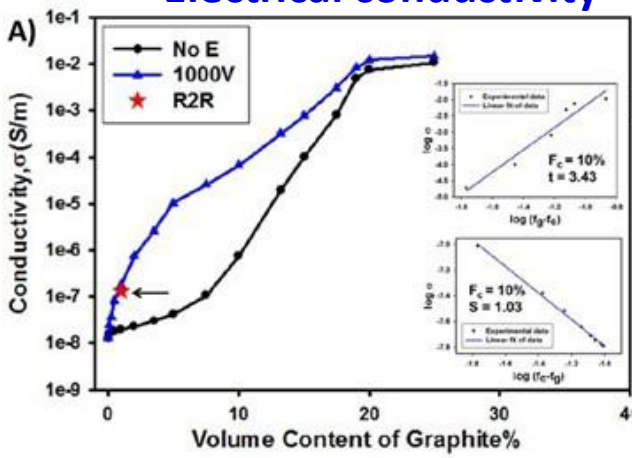

Thermal conductivity

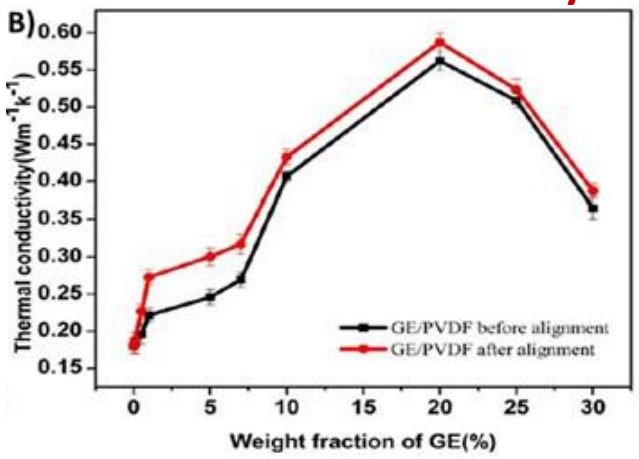

Aligned rGO sheets in LCE matrix

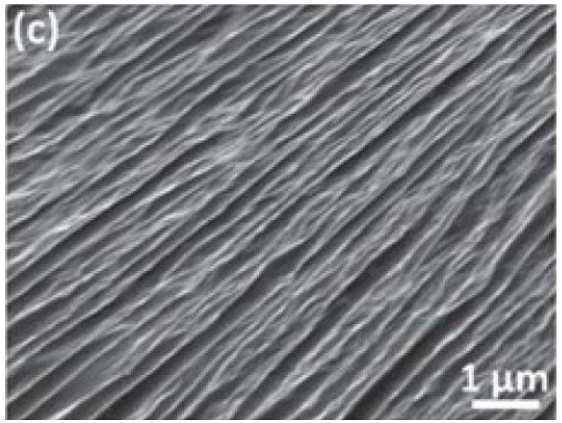

Randomly oriented rGO sheets in LCE matrix

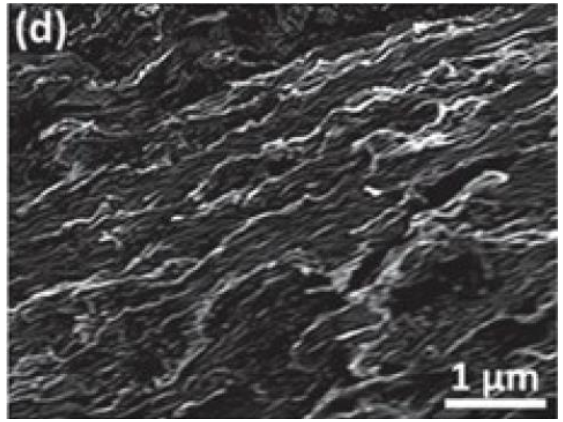

rGO peak at 3443 cm^{-1}

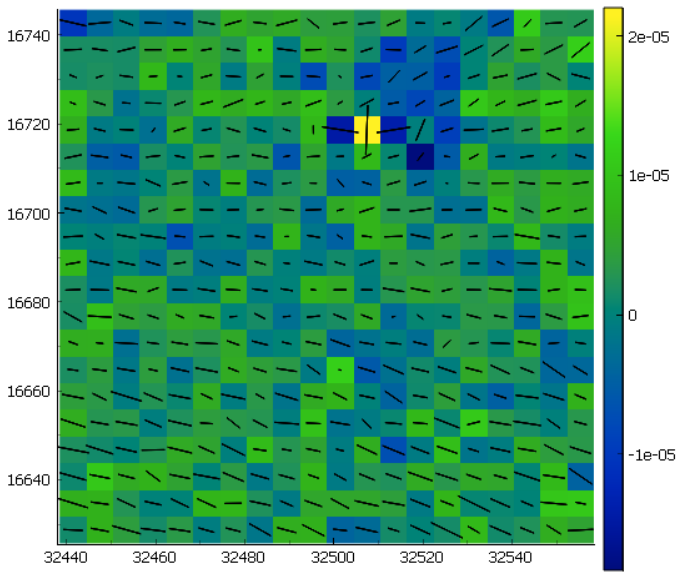

rGO peak at 3443 cm^{-1}

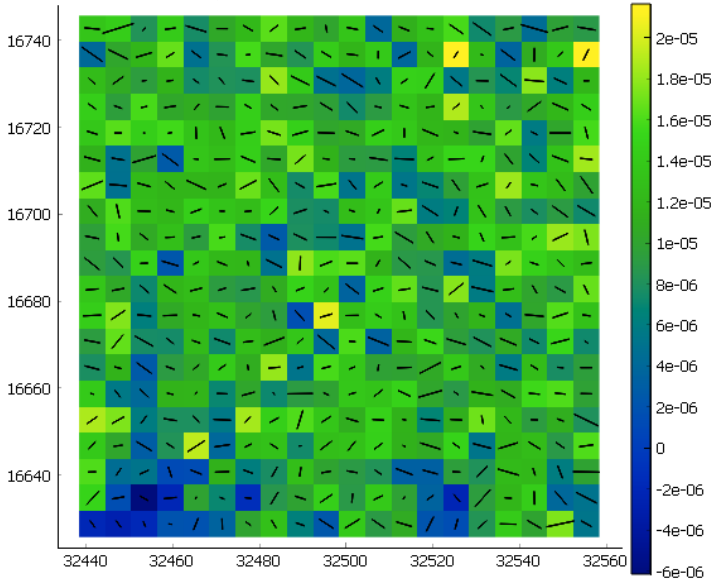

Ref: J. Ince, A. Al-qatatsheh, **J. Vongsvivut**, S. Juodkazis, N. Hameed, N. Salim, "Characterization of electrically aligned reduced graphene oxide sheets in liquid crystalline elastomer matrices," *manuscript in preparation*.

TRANSMISSION 5

Insights into changes of molecular orientation in scissor-like two-directional deformation of *Ferroelastic Organic Crystals* (FEOCs) during compression

SWINBURNE UNIVERSITY OF TECHNOLOGY

Tokyo Institute of Technology

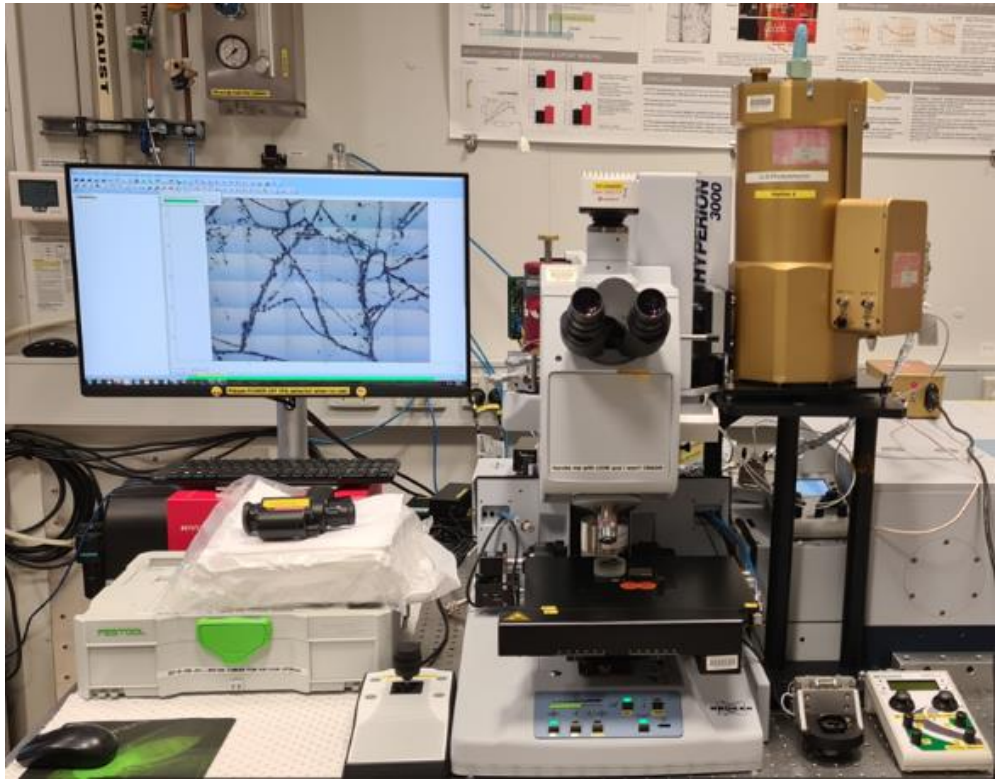

Coupling Si:B photodetector on IRM's FTIR microscope

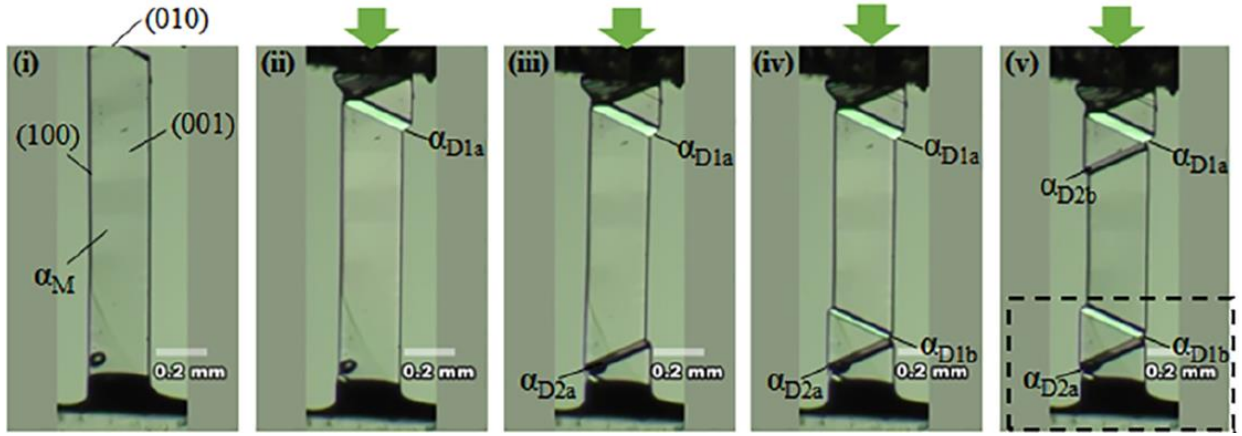

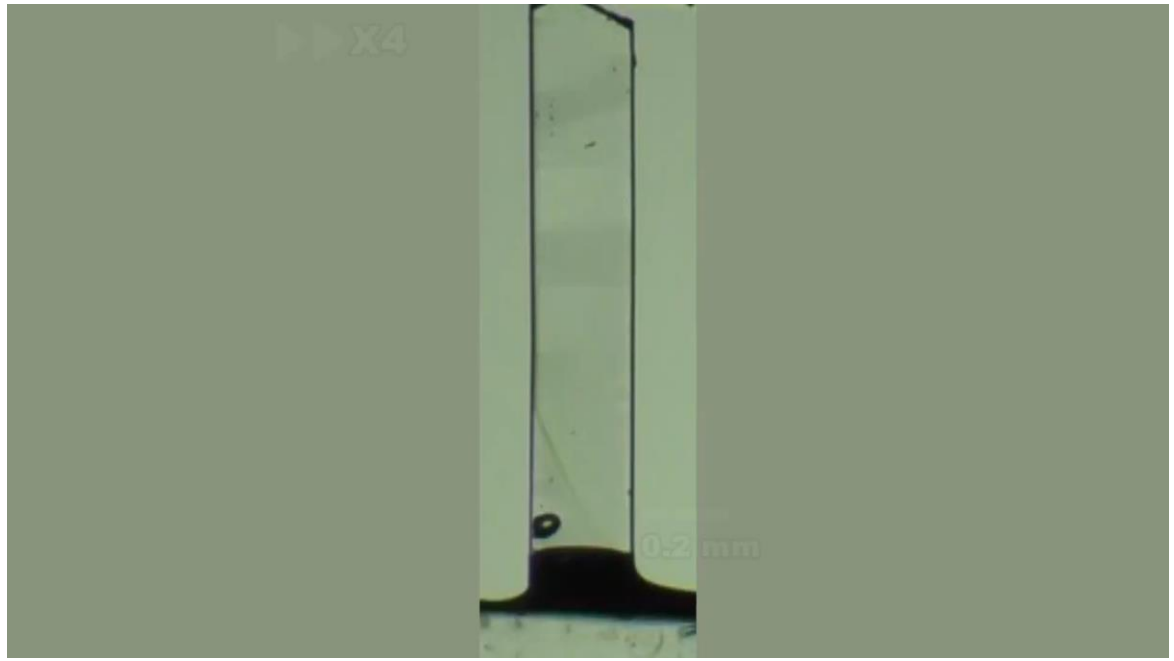

Ref: S. Ranjan, M. Ryu, R. Morioka, S. Kamegaki, S. H. Ng, D. Smith, **J. Vongsvivut**, **M. J. Tobin**, S. Juodkazis, J. Morikawa, and S. Takamizawa, "Structural and Thermal Diffusivity Analysis of an Organoferroelastic Crystal Showing Scissor-Like Two-Directional Deformation Induced by Uniaxial Compression," *J. Am. Chem. Soc.* (2023), **145**, *42*, 23027-23036 .

TRANSMISSION 5

Insights into changes of molecular orientation in scissor-like two-directional deformation of *Ferroelastic Organic Crystals* (FEOCs) during compression

SWINBURNE UNIVERSITY OF TECHNOLOGY

Tokyo Institute of Technology

Average transmission spectra of *Ferroelastic Polymer* at different polarisation angles

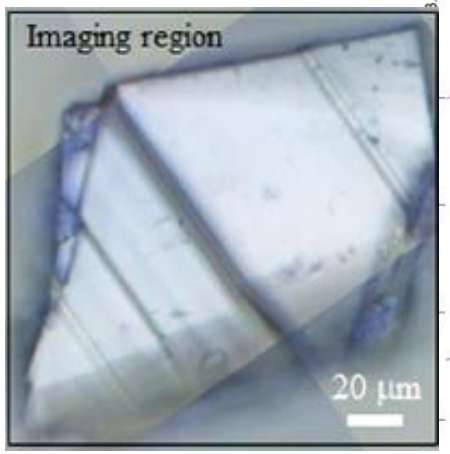

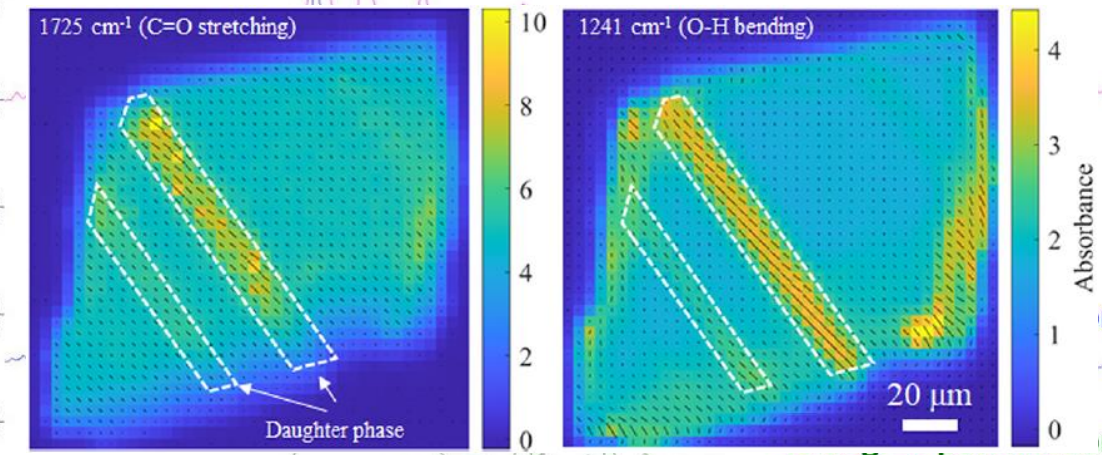

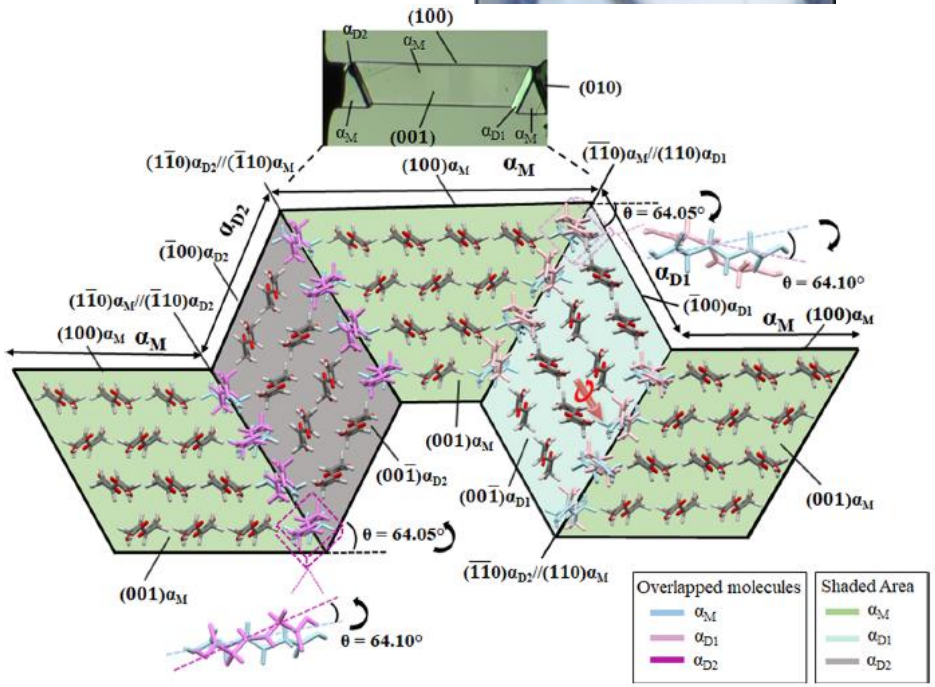

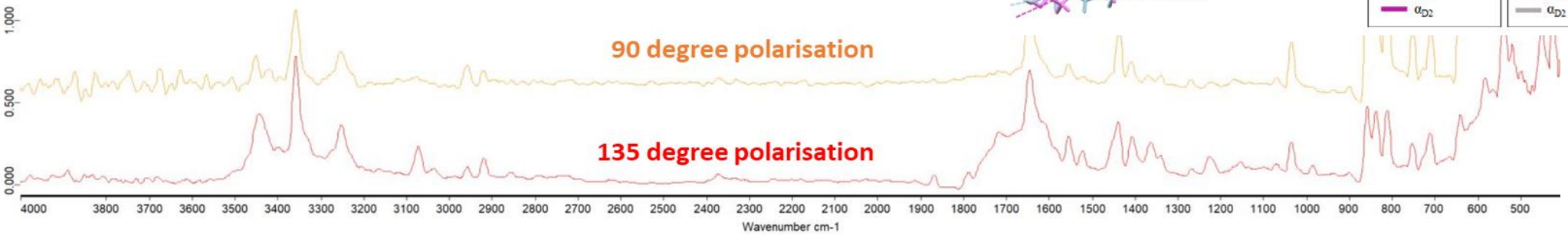

Ref: S. Ranjan, M. Ryu, R. Morioka, S. Kamegaki, S. H. Ng, D. Smith, **J. Vongsvivut**, **M. J. Tobin**, S. Juodkazis, J. Morikawa, and S. Takamizawa, "Structural and Thermal Diffusivity Analysis of an Organoferroelastic Crystal Showing Scissor-Like Two-Directional Deformation Induced by Uniaxial Compression," *J. Am. Chem. Soc.* (2023), **145**, *42*, 23027-23036 .

Traditional Sampling Methods

– *Reflectance* for In-Situ Catalysis Reactions –

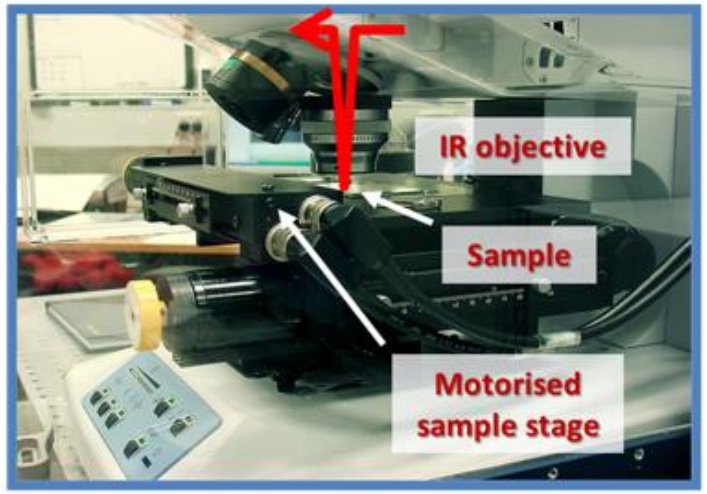

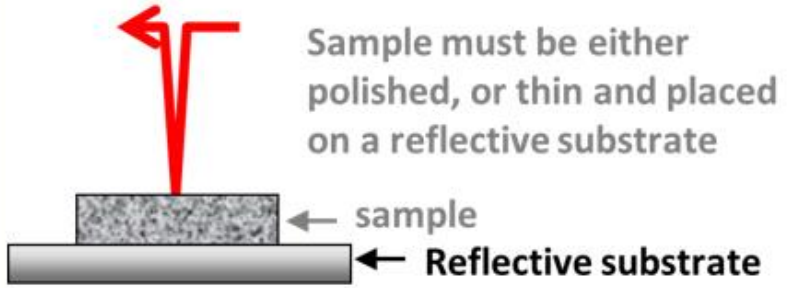

ANSTO

REFLECTANCE ❶ In-situ monitoring of anti-freezing electrolytes for aqueous Zn battery

THE UNIVERSITY of ADELAIDE

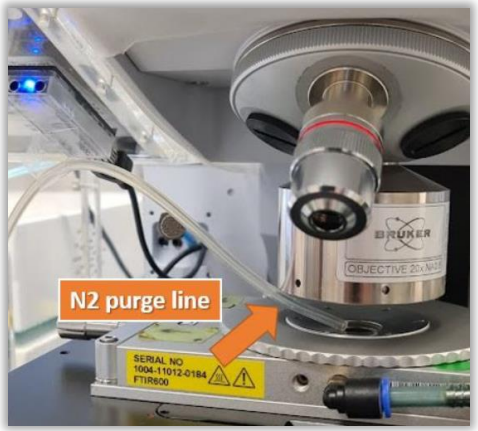

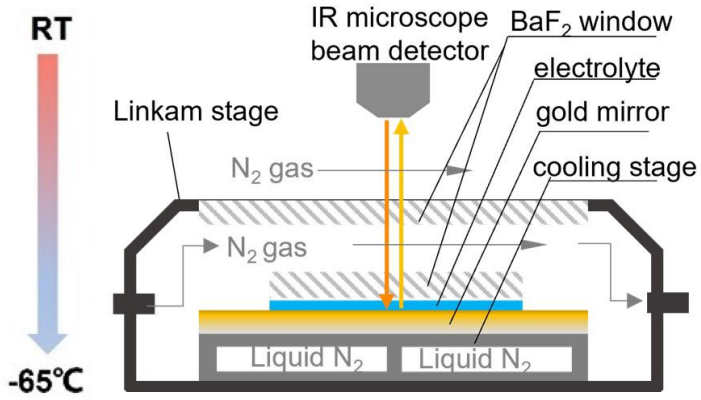

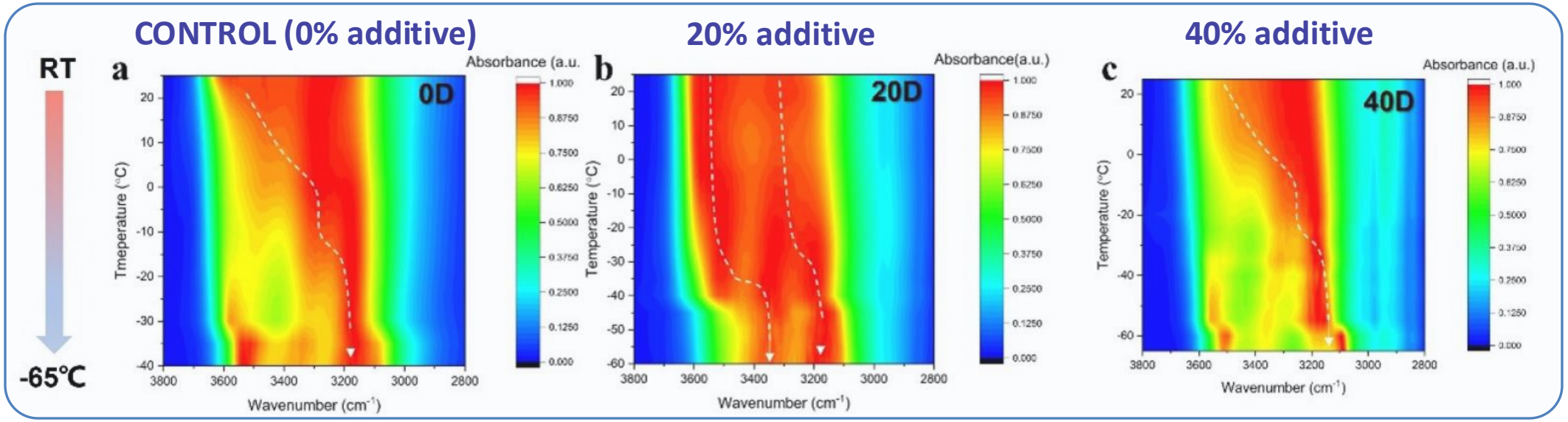

- **Changes of intensity at different wavenumbers across the temperature range suggest altered interactions between the additives and co-solvents at the sub-zero conditions,** leading to a new understanding of their anti-freezing mechanism(s).

REFLECTANCE 2

UNSW SYDNEY

Gaining insights into reaction mechanism of photoelectrochemical urea synthesis using *in-situ* synchrotron-FTIR technique

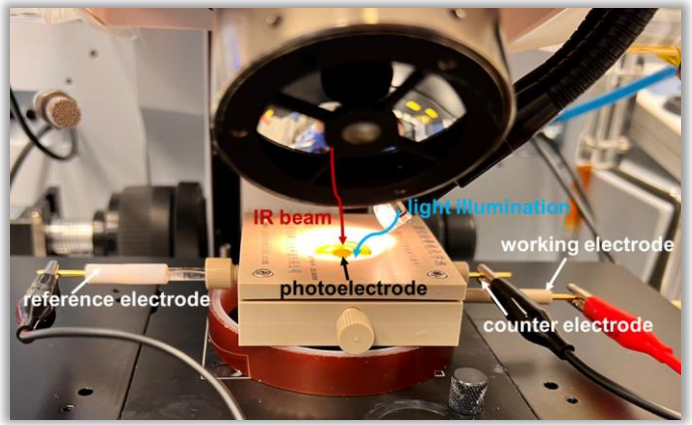

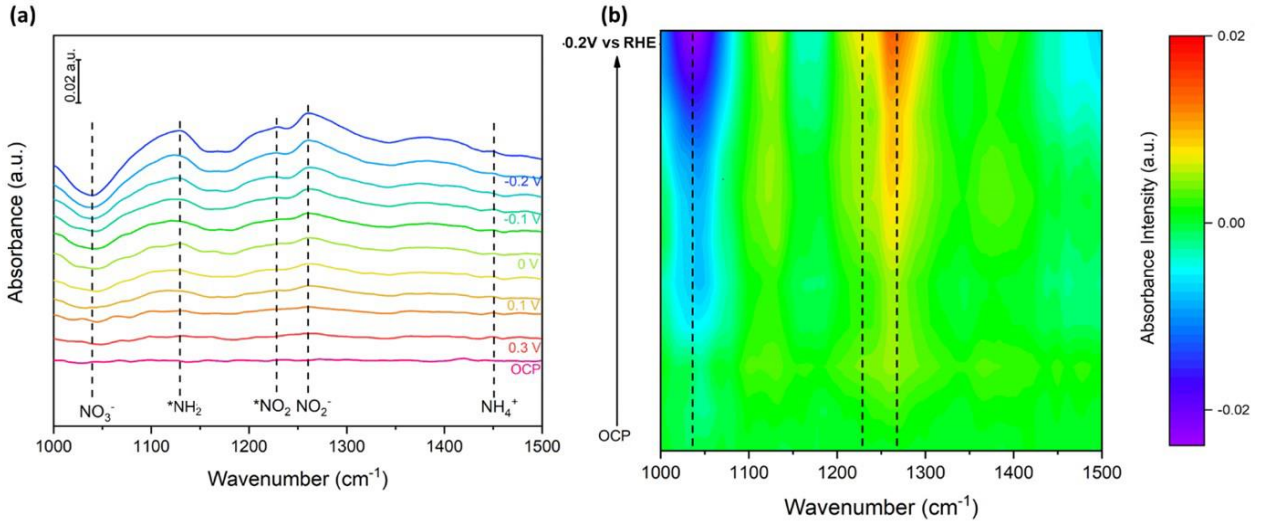

- **Spectral series collected over a range of applied voltage revealed the production of nitrogen intermediates over the course of the reaction that led to insights into the mechanism,** important for optimizing the production and yields.

Ref [1]: C. Han *et al.*, "Nanostructured Hybrid Catalysts Empower the Artificial Leaf for Solar-Driven Ammonia Synthesis" *Energy Environ. Sci.* (2024), **17**, 5653-5665.
Ref [2]: S. Zhou *et al.*, "Solar driven Ammonia Synthesis with Co-TiO_x and Ag Nanowires Enhanced Cu_2ZnSnS_4 Photocathodes" *Appl. Catal. B.* (2024), **348**, 123836.

In-house Developed

Hybrid Macro ATR-FTIR Technique

– Recent Highlighted Applications –

ANSTO

OVERVIEW

Background "Macro-ATR" → **Macro-ATR Devices** → **Applications**

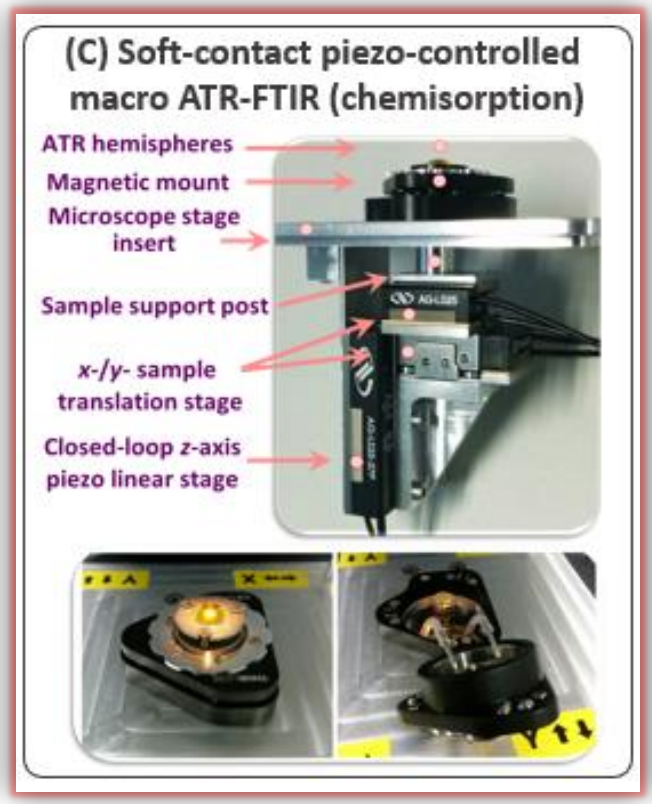

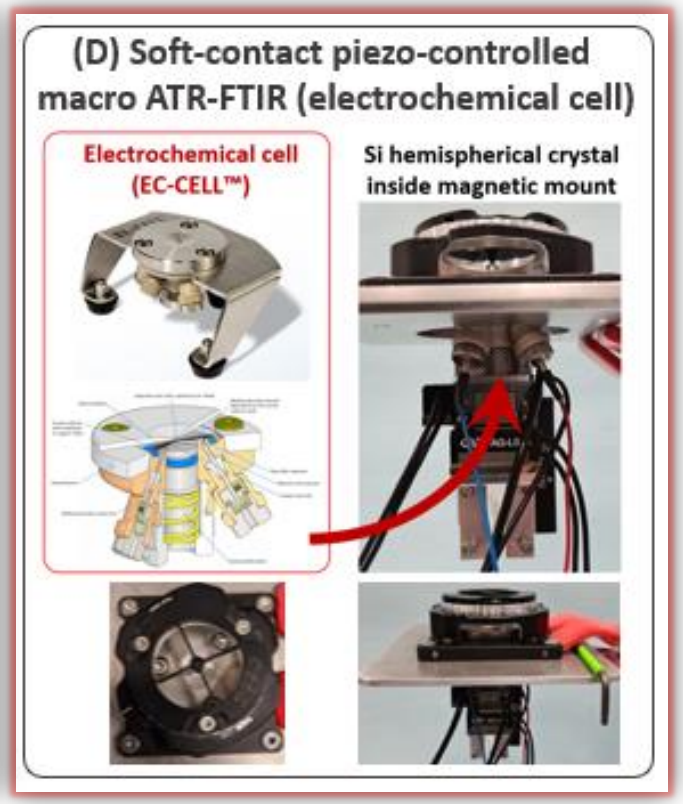

Ref: **J. Vongsvivut**, D. Perez-Guaita, B.R. Wood, P. Heraud, K. Khambatta, D. Hartnell, M. Hackett, **M.J. Tobin**, "Synchrotron macro ATR-FTIR microspectroscopy for high-resolution chemical mapping of single cells," *Analyst* (2019) **144**, 3226-3238.

PRINCIPLE OF (MACRO) ATR-FTIR SPECTROSCOPY

ATR-FTIR utilizes **TOTAL INTERNAL REFLECTION** phenomenon when IR radiation travels through high index ATR crystal and impinges on low-index sample surface at $\theta_{incident} > \theta_c$ resulting in evanescent wave, which decays exponentially into sample surface (d_p).

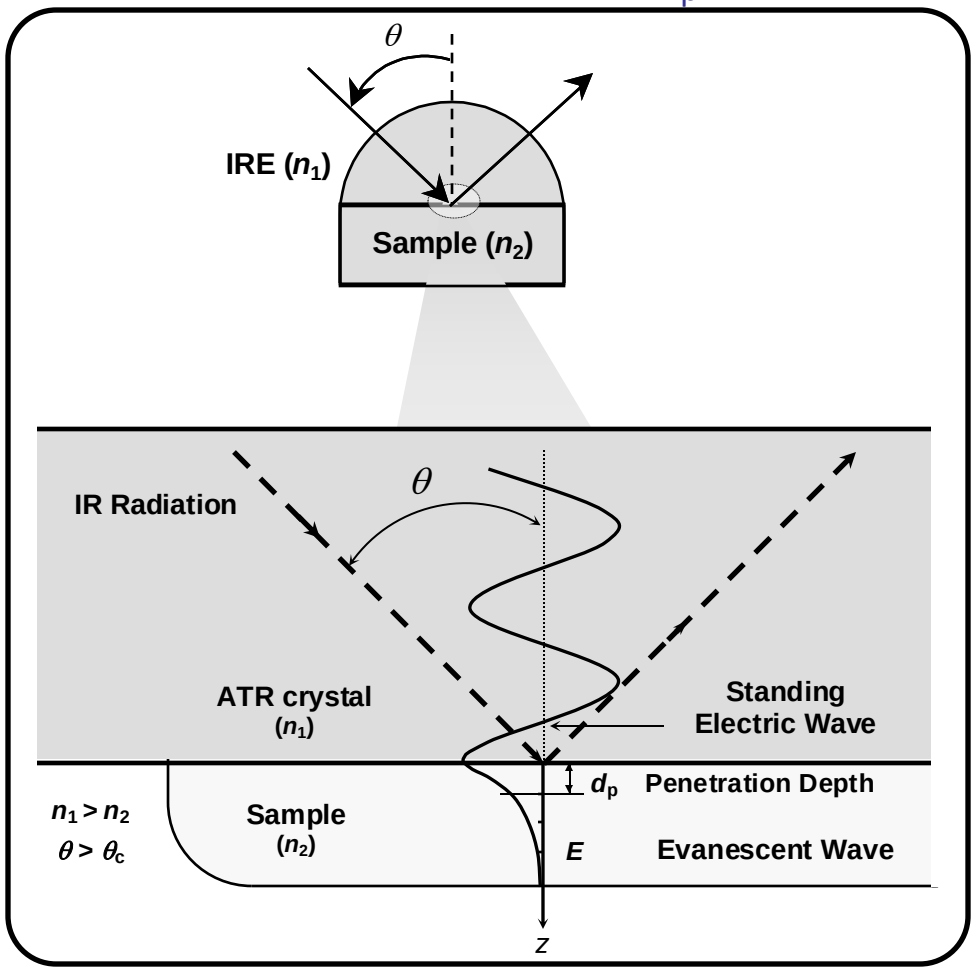

spatial resolution with total internal reflection

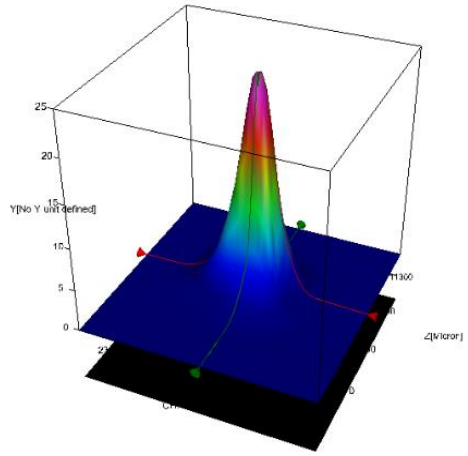

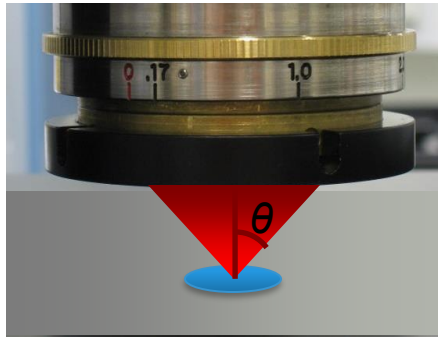

Rayleigh Equation:

$r = 1.22\ \lambda\ /\ 2 \times$ ***NA***

Numerical aperture

NA = n(sinθ)

At λ = 6 µm

For *NA* (air) = 0.65

r = 5.6 µm (TRANS & REFL)

At λ = 6 µm

For *NA* (ZnSe) = 1.56

r = 2.3 µm

At λ = 6 µm

For *NA* (Ge) = 2.6

r = 1.4 µm (Ge ATR)

Ref: J. Vongsvivut *et al.* Rapid determination of protein contents in microencapsulated fish oil supplements by ATR-FTIR spectroscopy and partial least square regression (PLSR) analysis, *Food Bioprocess Technol.* (2013) **7**, 265-277.

TRADITIONAL MICRO-ATR TECHNIQUE

Commercial Bruker ATR 20× objective equipped with Ge-ATR crystal

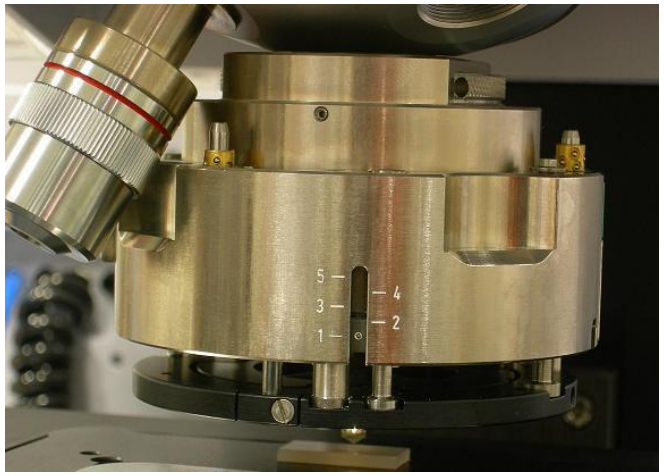

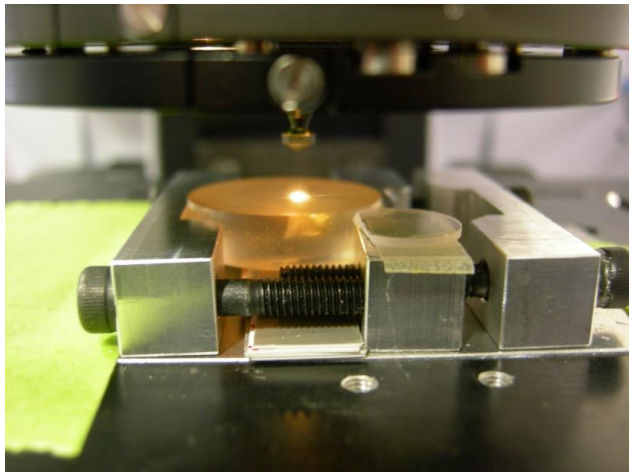

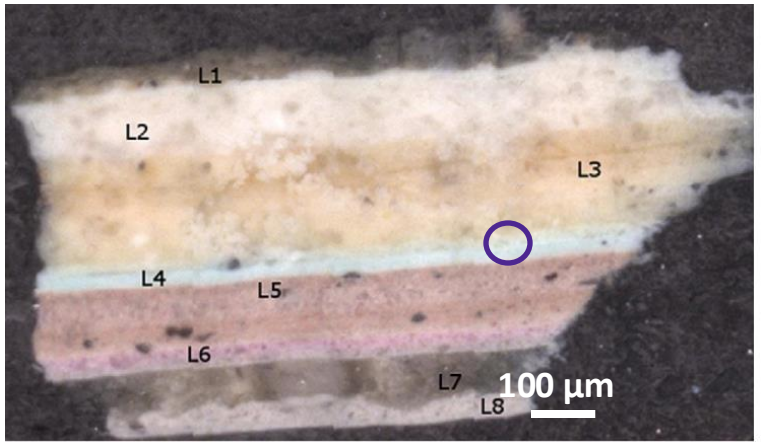

Multilayer paint fragment from exterior of Provincial Hotel (Fitzroy). Sample was not suitable for thin sectioning.

☹

- × Sample damage
- × Contamination
- × Slow scan

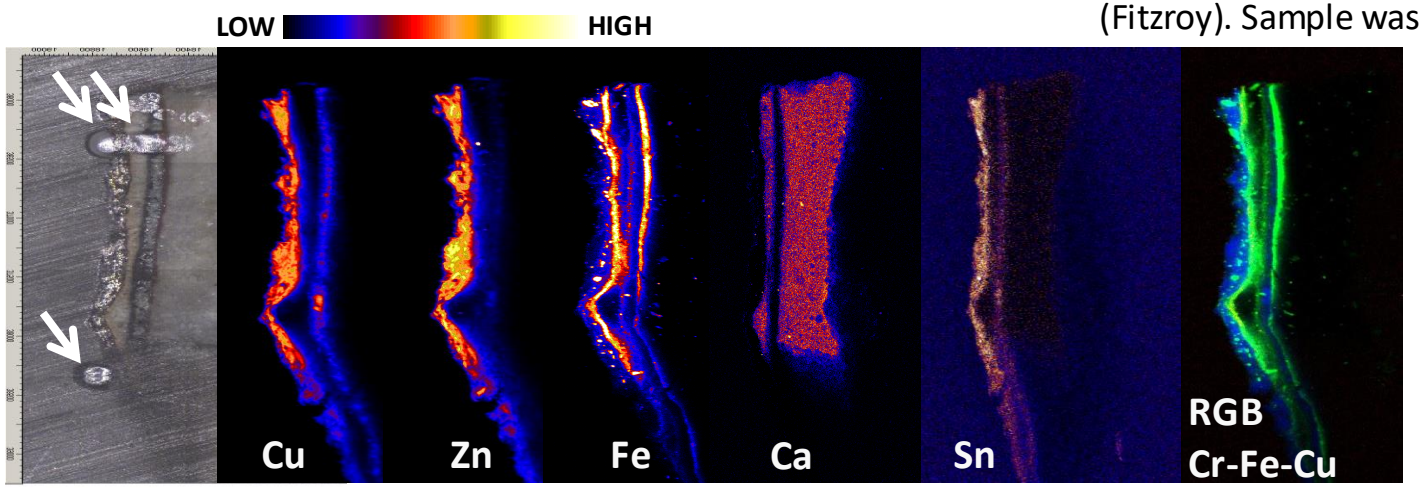

Visible image of a paint cross section recorded after standard micro-ATR "mapping" measurements (*left*), showing indentation marks damaged by the high pressure from the ATR crystal (*arrowed*)

Ref: R. Sloggett *et al.* Microanalysis of artworks: IR microspectroscopy of paint cross-sections, *Vib. Spectrosc.* (2010) **53**, 77-82.

ANSTO

MODEL 1: "HYBRID" MACRO-ATR WITH 20× OBJECTIVE

Bruker Macro-ATR unit and setup

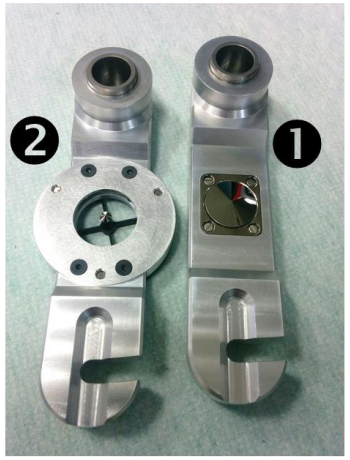

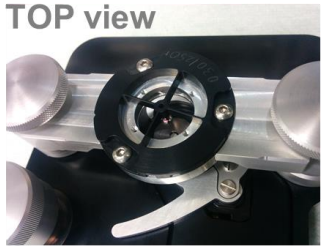

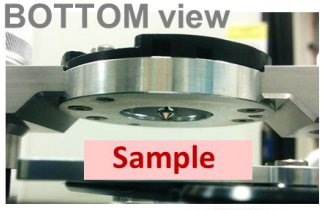

MACRO-ATR cantilever arm:

250-μm-dia tip

❶ **ORIGINAL model** supplied with 1-mm-dia facet Ge crystal.

❷ **HYBRID version:** in-house modification to accept 250-μm-dia and 100-μm-dia facet Ge crystals from commercial micro-ATR objectives.

Non-contact position for background measurement

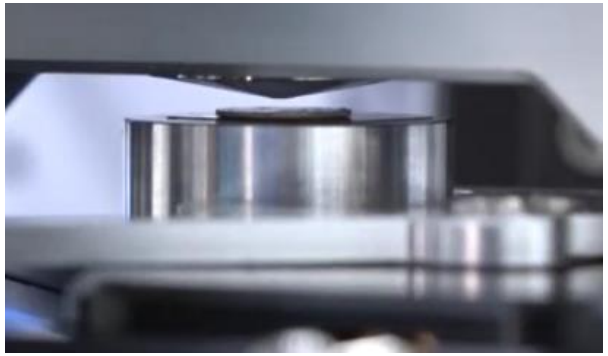

Contact position for mapping measurement

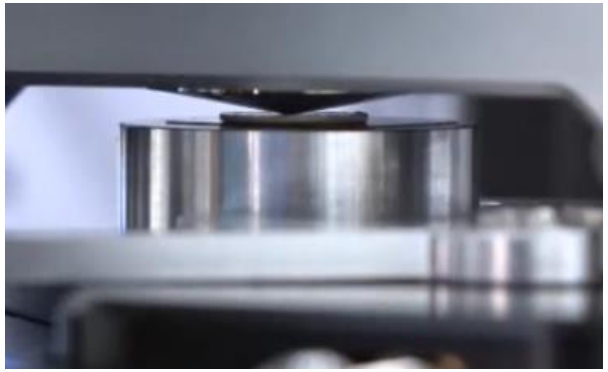

- ✓ No cross contamination
- ✓ Faster scan
- ✓ Minimal sample damage

Available sizes of Ge facet tip: 1 mm, 250 μm and 100 μm offering a good range of contact pressure on samples.

Ref: V.K. Truong *et al.* Evolution of silica nanoparticle-polyester coatings on surfaces exposed to sunlight, *J. Vis. Exp.* (2016) **116**, e54309.

MODEL 1: "HYBRID" MACRO-ATR WITH 20× OBJECTIVE

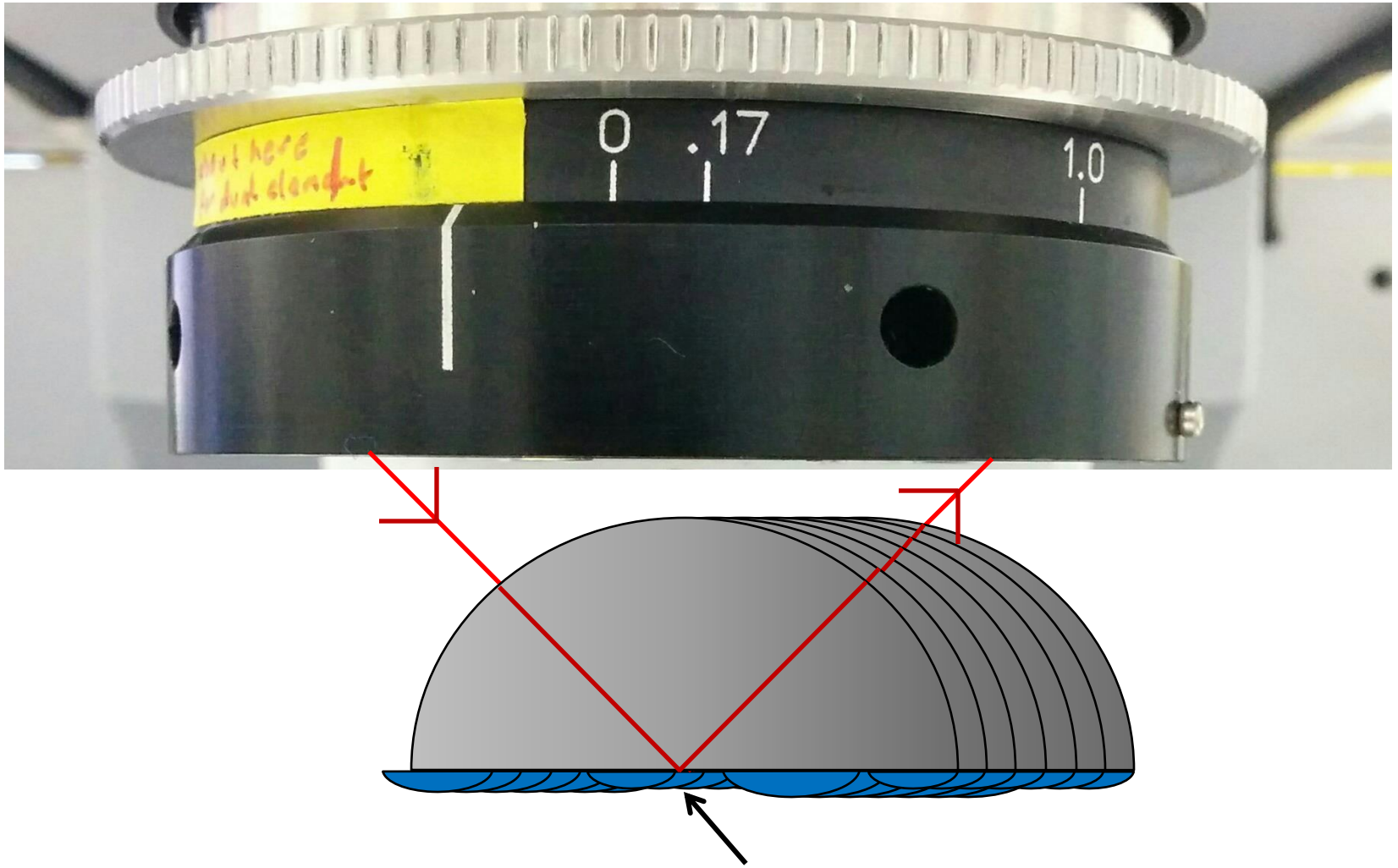

Step interval of the beam between measurement points is also reduced by a factor of 4 for Ge crystal (n_{Ge} = 4)

smallest projected aperture available ~1 μm | smallest step (lateral) resolution = 250 nm

MACRO-ATR 1

Flinders University

Plasma jet transforms blue-green *Spirulina* microalgae into ultrathin bioactive coatings for anti-bacterial wound healing applications (Patent No. AU2023902971)

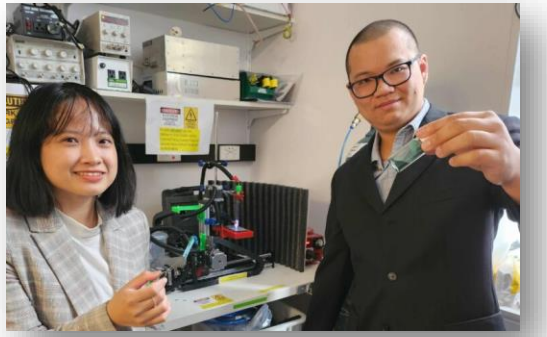

Blue-green *Spirulina* microalgae

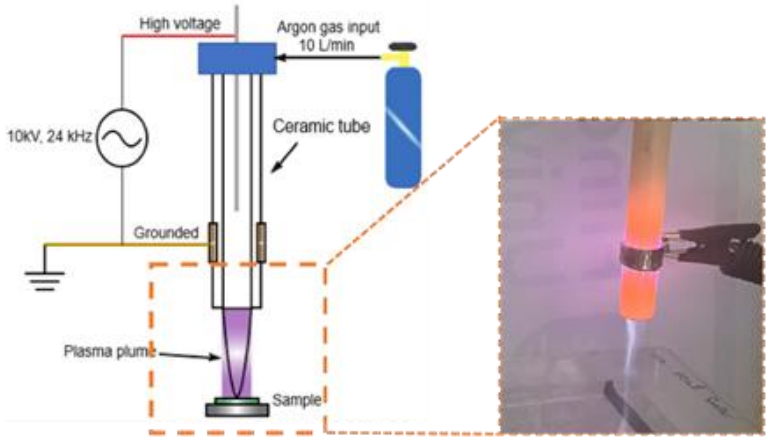

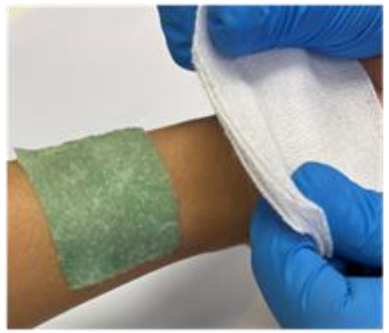

Synchrotron Macro-ATR analysis

Antibacterial and antibiofilm

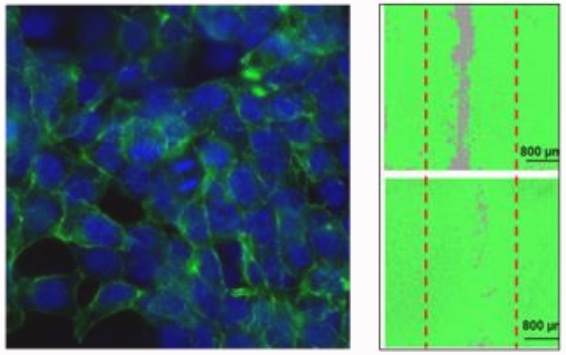

Wound healing

- **Argon plasma jet technique:** an innovative sustainable approach to harness antibacterial compound "phycocyanin" by breaking down *Spirulina* cell wall creating uniform bioactive coating on the surface of the substrate *in just one single step*.

Ref: T. T. Nguyen, N. H. Nguyen, A. Hayles, W. Li, D. Q. Pham, C. K. Nguyen, T. Nguyen, **J. Vongsvivut**, N. Ninan, Y. Sabri, W. Zhang, K. Vasilev, V. K. Truong, "Transforming *Spirulina maxima* Biomass into Ultrathin Bioactive Coatings Using an Atmospheric Plasma Jet – A New Approach to Healing of Infected Wounds," *Small* (2023) **2305469**.

MACRO-ATR 1

Flinders University

Plasma jet transforms blue-green *Spirulina* microalgae into ultrathin bioactive coatings for anti-bacterial wound healing applications (Patent No. AU2023902971)

Scanning Electron Microscope

Control (untreated)

Plasma treated (100 s/cm²)

Plasma treated (200 s/cm²)

Synchrotron Macro ATR-FTIR technique

Control Plasma-treated Principal Component Analysis (PCA)

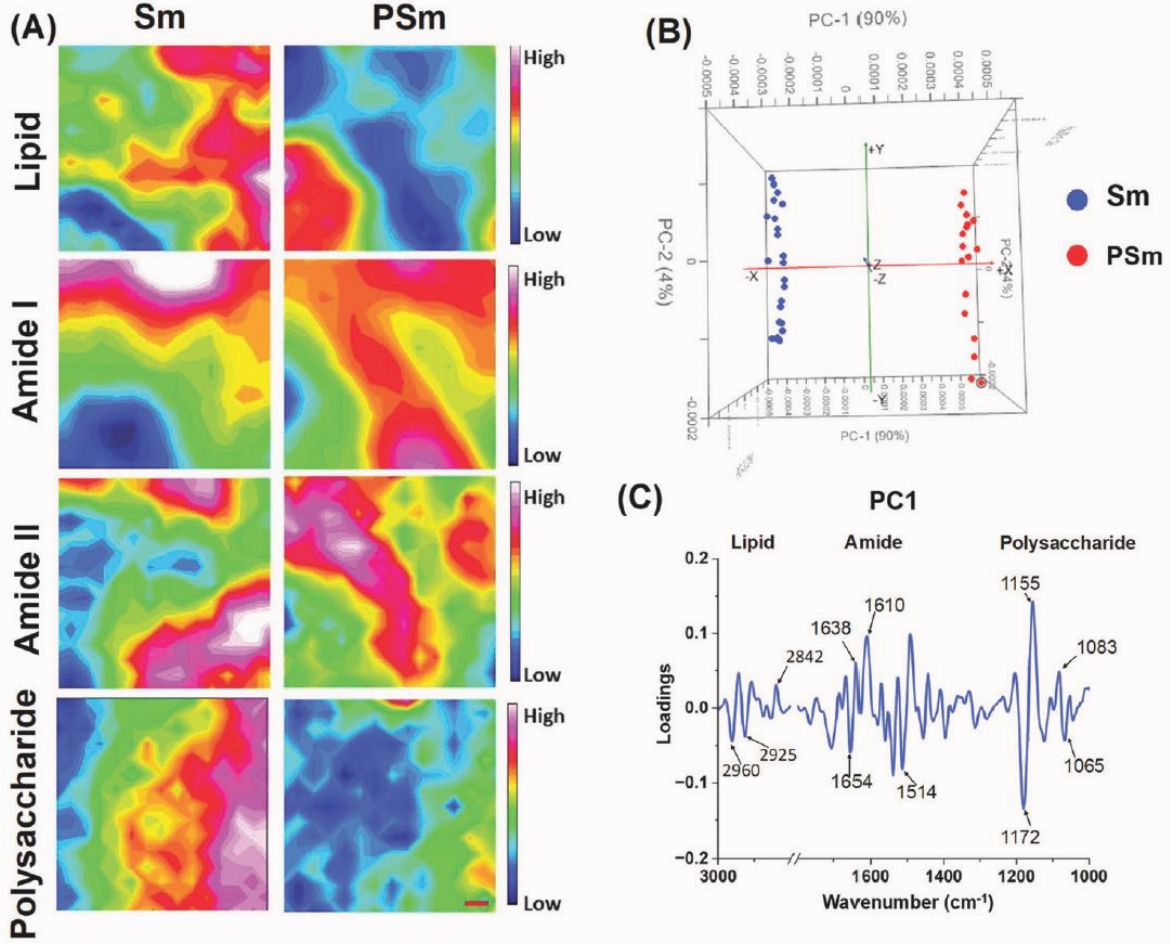

Ref: T. T. Nguyen, N. H. Nguyen, A. Hayles, W. Li, D. Q. Pham, C. K. Nguyen, T. Nguyen, **J. Vongsvivut**, N. Ninan, Y. Sabri, W. Zhang, K. Vasilev, V. K. Truong, "Transforming *Spirulina maxima* Biomass into Ultrathin Bioactive Coatings Using an Atmospheric Plasma Jet – A New Approach to Healing of Infected Wounds," *Small* (2023) **2305469**.

MACRO-ATR 2

UNSW SYDNEY

Investigating surface composition and encapsulation stability of novel β-carotene microcapsules produced using pea/whey protein complexes

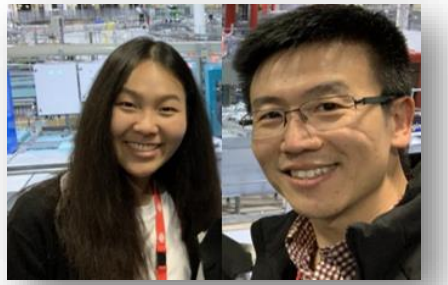

Control
(pea/whey protein blends)

TG-MD
(cross-linked pea/whey protein blends + maltodextrin)

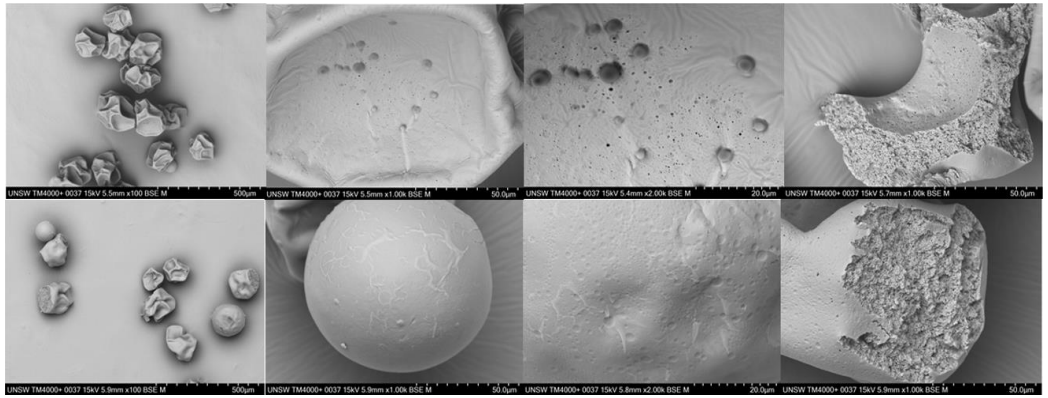

Encapsulation efficiency over 8 weeks

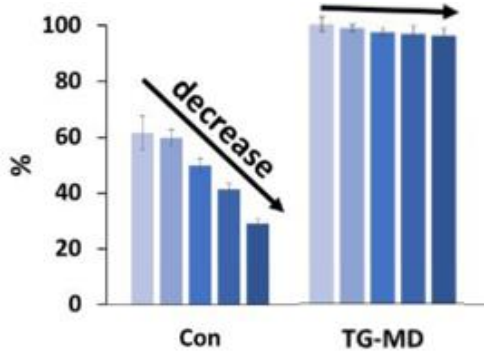

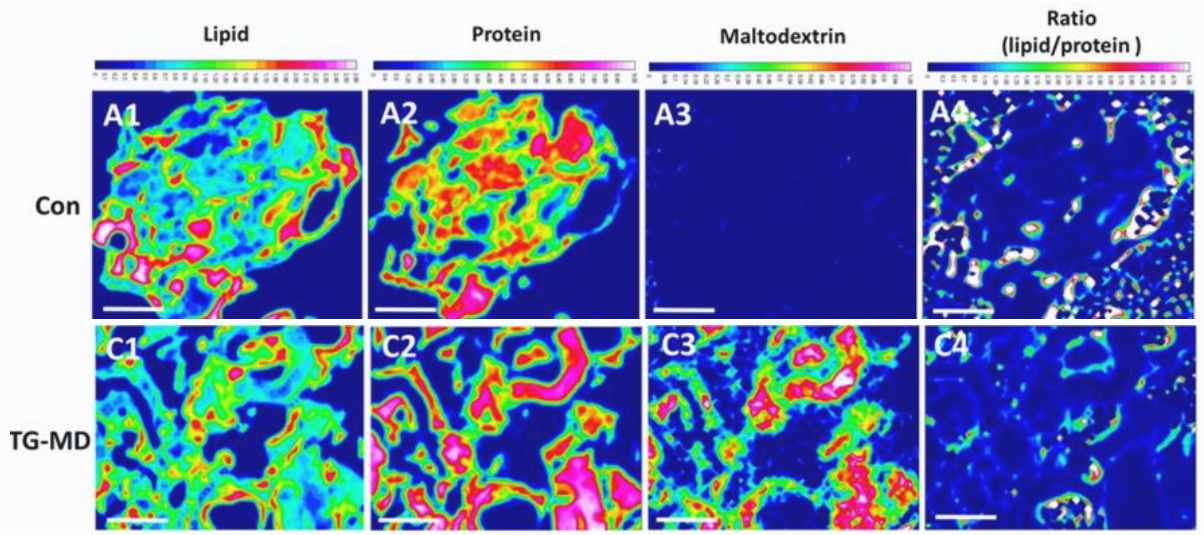

Surface composition (lipid:protein ratio)

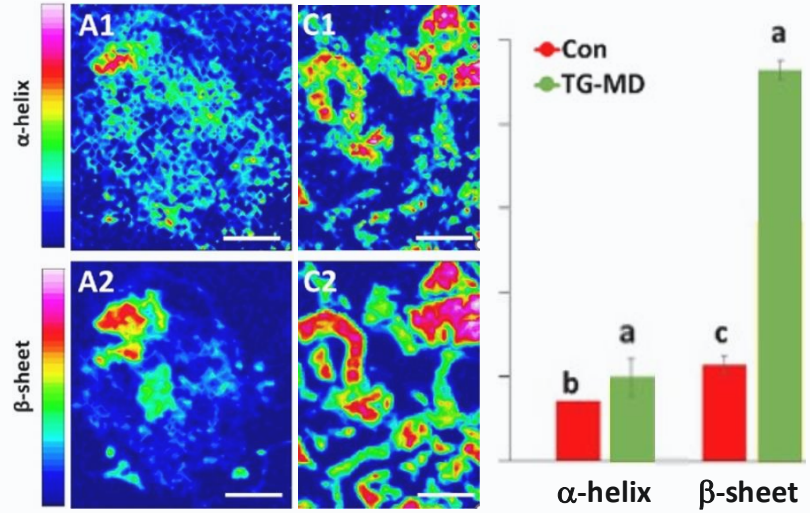

Protein secondary structure

Ref: W. Kim, Y. Wang, **J. Vongsvivut**, Q. Ye, C. Selomulya, "On Surface Composition of β-Carotene Microcapsules Comprising Pea/Whey Protein Complexes by Synchrotron-FTIR Microspectroscopy," *Food Chem.* (2023) **426**, 136565.

In-House Developed

Piezo-Controlled Macro ATR-FTIR Technique

– Current Progress in Battery Research –

ANSTO

PIEZO-ATR ❶

In-operando monitoring of electrochemical reaction on Zn electrode

THE UNIVERSITY of ADELAIDE

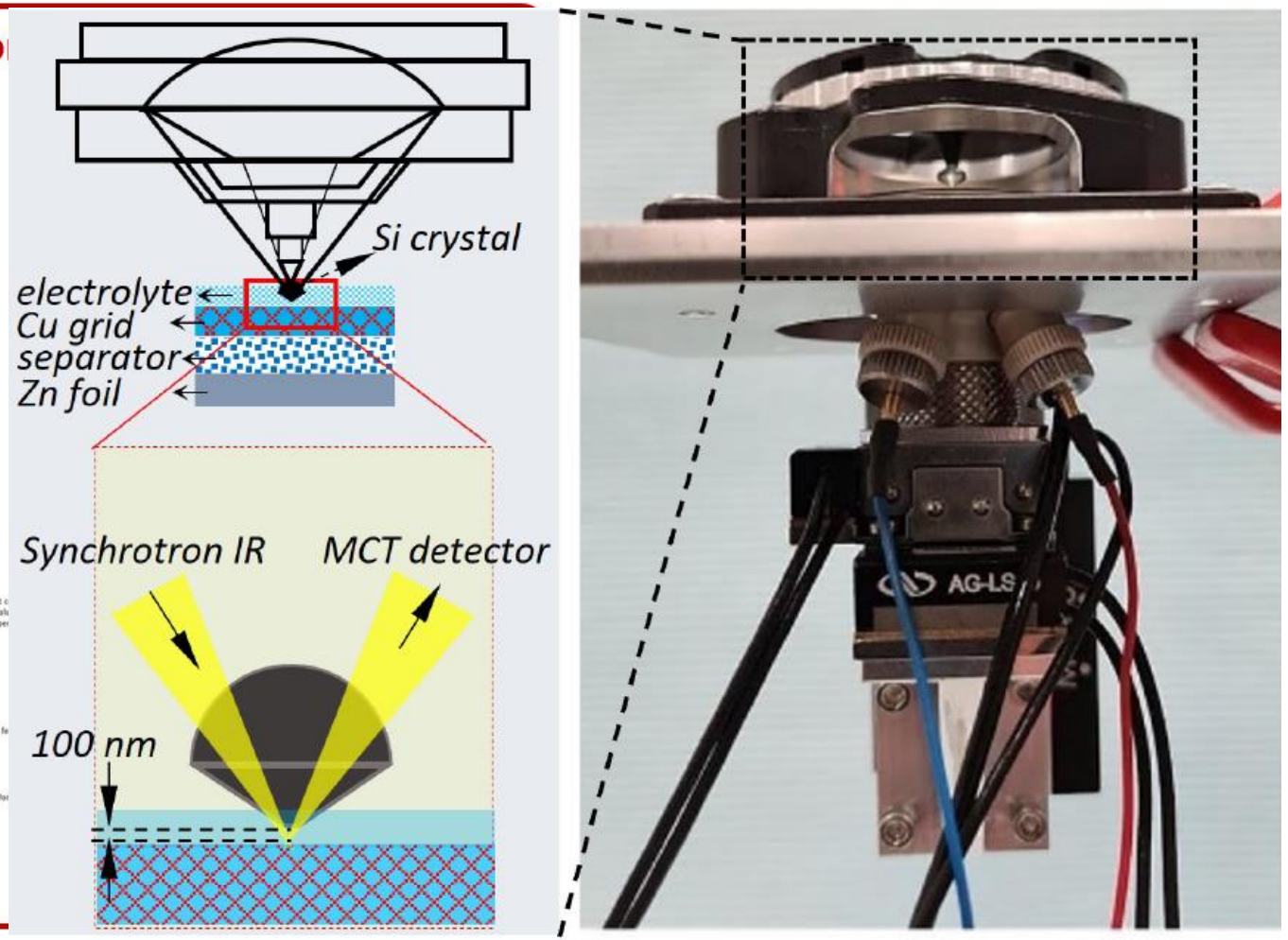

The success on observing the intensity changes of solvent (DMMP) and anion (Otf^-) during electrochemical reactions

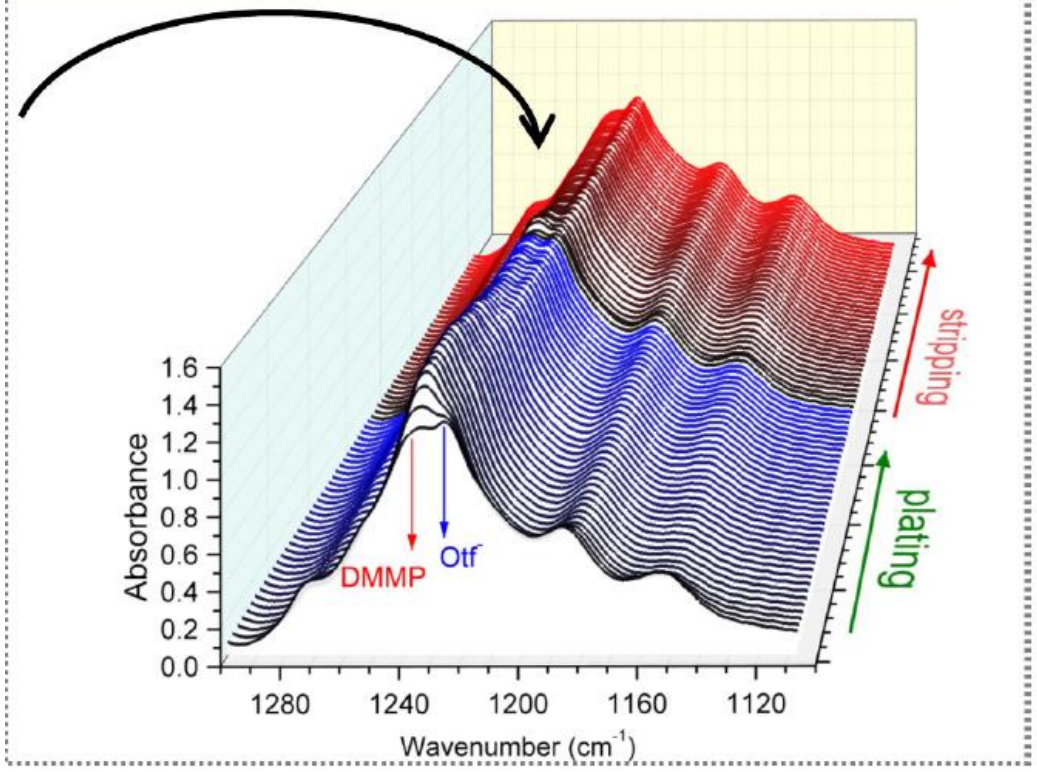

Ref: **S. Liu**, **J. Vongsvivut**, Y. Wang, R. Zhang, F. Yang, S. Zhang, K. Davey, J. Mao, and Z. Guo, "Monolithic Phosphate Interphase for Highly Reversible and Stable Zn Metal Anode," *Angew. Chem. Int. Ed.* (2023), **62**, *4*, e202215600.

PIEZO-ATR 1

In-operando monitoring of electrochemical reaction on Zn electrode

THE UNIVERSITY of ADELAIDE

Changes in relative intensity between salt anion and solvent suggested decomposing reaction of the electrolyte at the interface, useful for understanding interfacial reactions in the real battery!

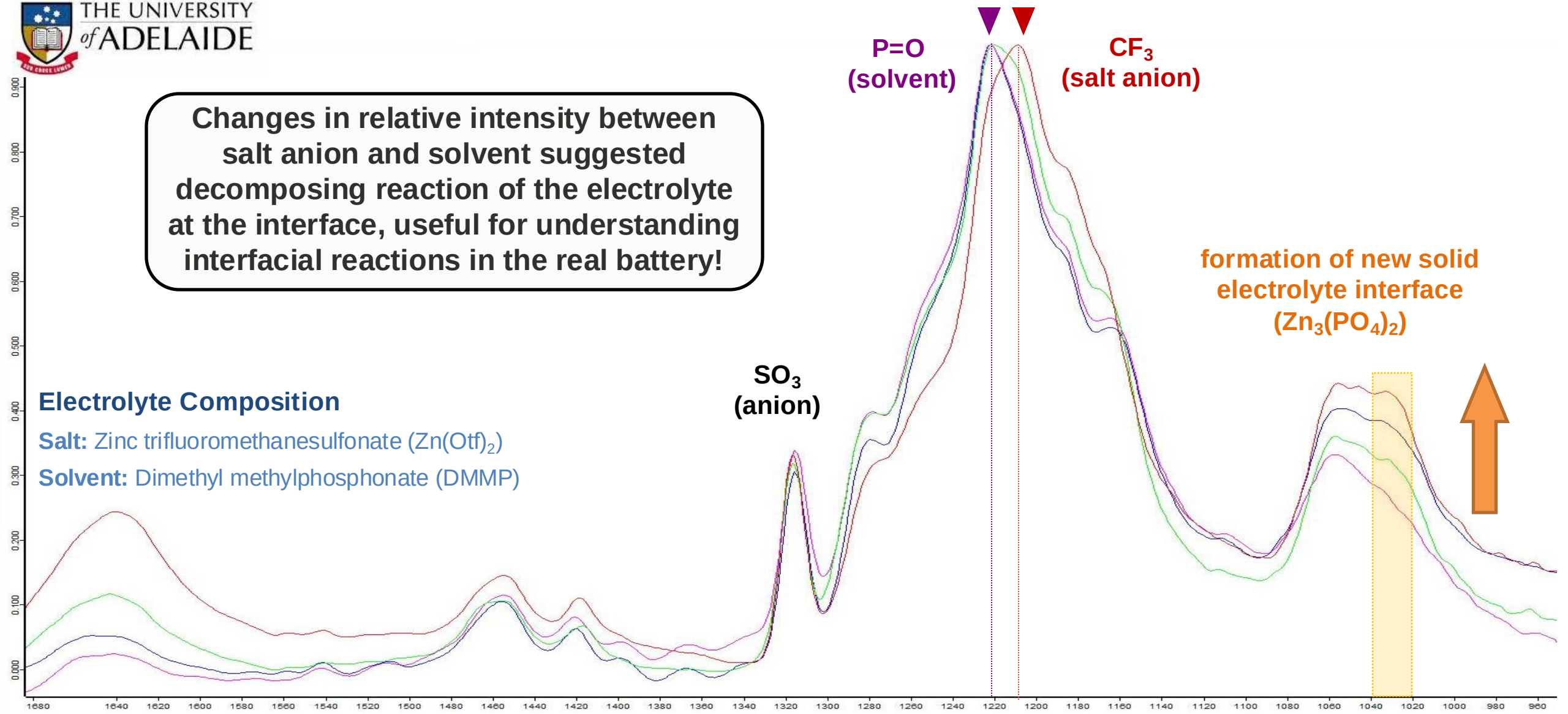

Electrolyte Composition

Salt: Zinc trifluoromethanesulfonate ($Zn(Otf)_2$)

Solvent: Dimethyl methylphosphonate (DMMP)

Ref: **S. Liu**, **J. Vongsvivut**, Y. Wang, R. Zhang, F. Yang, S. Zhang, K. Davey, J. Mao, and Z. Guo, "Monolithic Phosphate Interphase for Highly Reversible and Stable Zn Metal Anode," *Angew. Chem. Int. Ed.* (2023), **62**, *4*, e202215600.

PIEZO-ATR 2

Biocompatible electrolytes for highly reversible Zn anode in Zn battery

THE UNIVERSITY of ADELAIDE

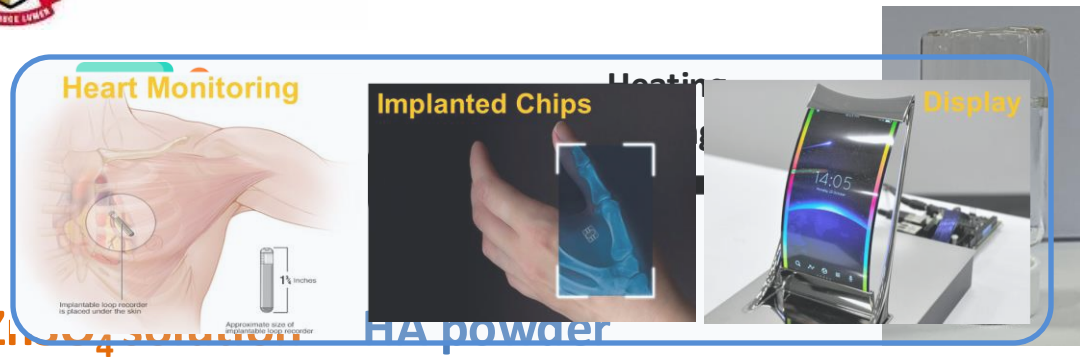

Superior performance of HA electrolyte (over liquid electrolyte):

- ✓ Long life span (~5,500 hours = 230 days)
- ✓ High Coulombic efficiency (99.71% high reversible)
- ✓ Wider electrochemical stable window (ESW)
- ✓ Good anti-corrosion property (i.e. negligible by-products generated)
- ✓ More uniform growth of Zn deposition
- ✓ Excellent flexibility to be made for flexible battery applications

Flexible zinc metal batteries

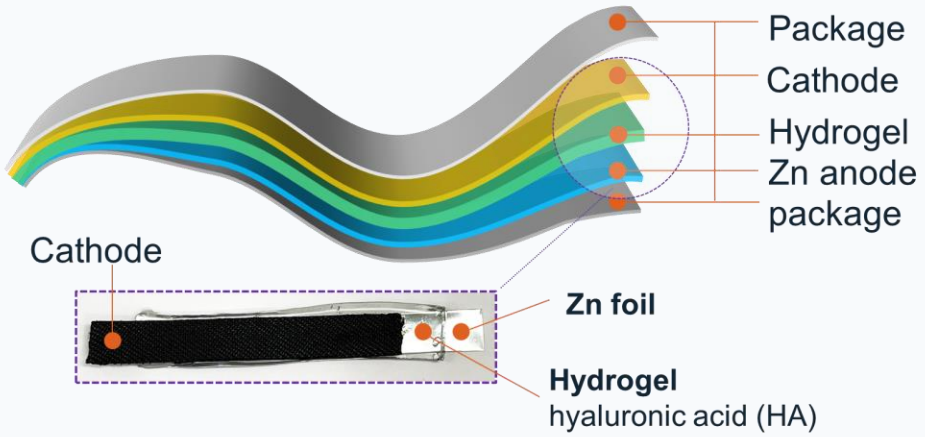

Good flexibility, non-flammable, low cost

Benchtop-FTIR: gaining insights into the electrochemical mechanism

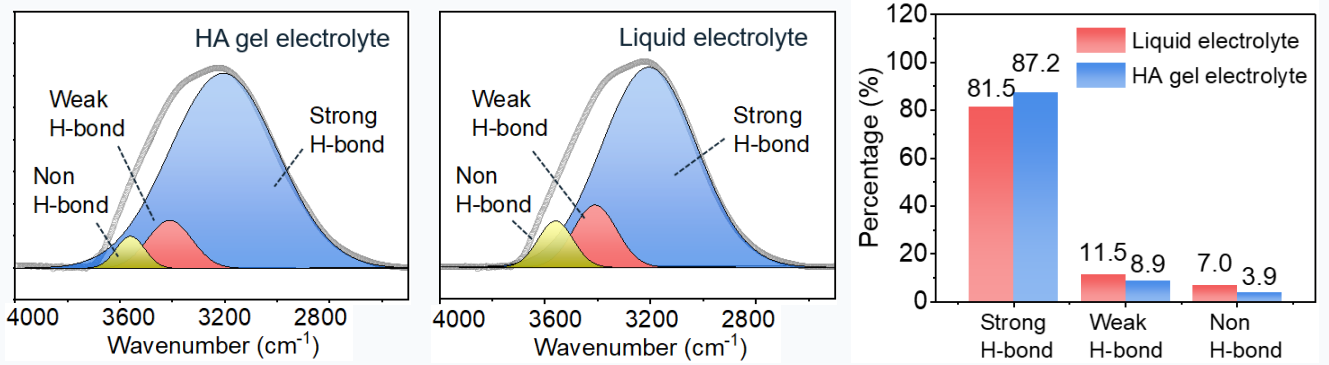

Ref: **G. Li**, Z. Zhao, S. Zhang, L. Sun, M. Li, J. A. Yuwono, J. Mao, J. Hao, **J. Vongsvivut**, L. Xing, C.-X. Zhao, Z. Guo, "A Biocompatible Electrolyte Enables Highly Reversible Zn Anode for Zinc Ion Battery," *Nat. Comm.* (2023), **14**, *1*, 6526.

PIEZO-ATR 2

Biocompatible electrolytes for highly reversible Zn anode in Zn battery

THE UNIVERSITY of ADELAIDE

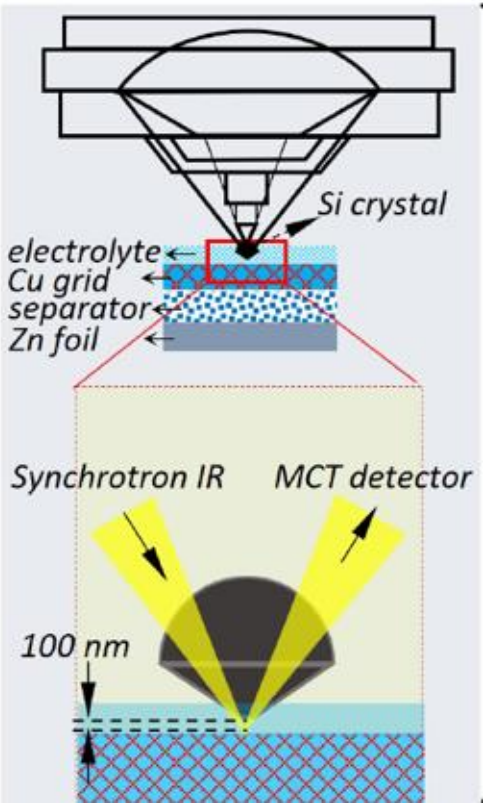

HA gel electrolyte

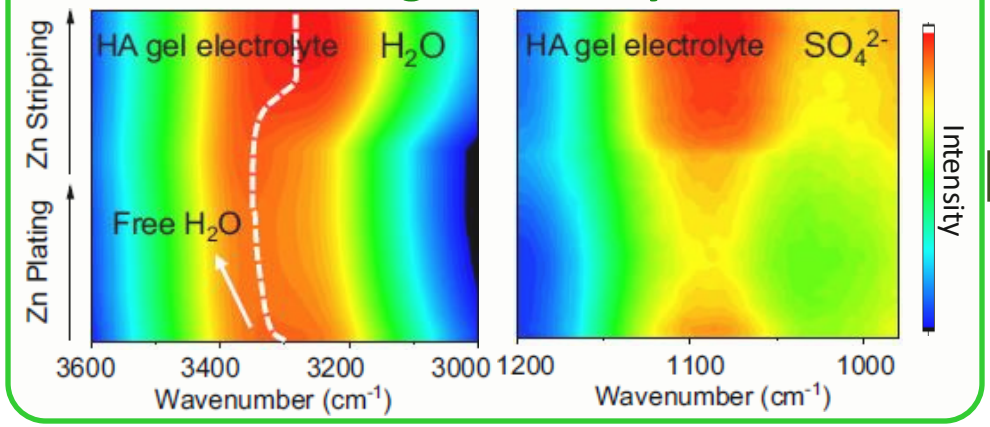

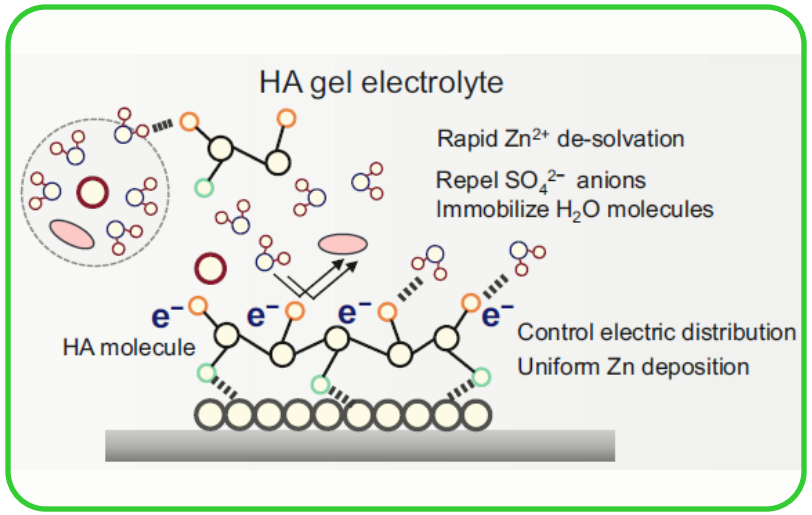

Liquid electrolyte

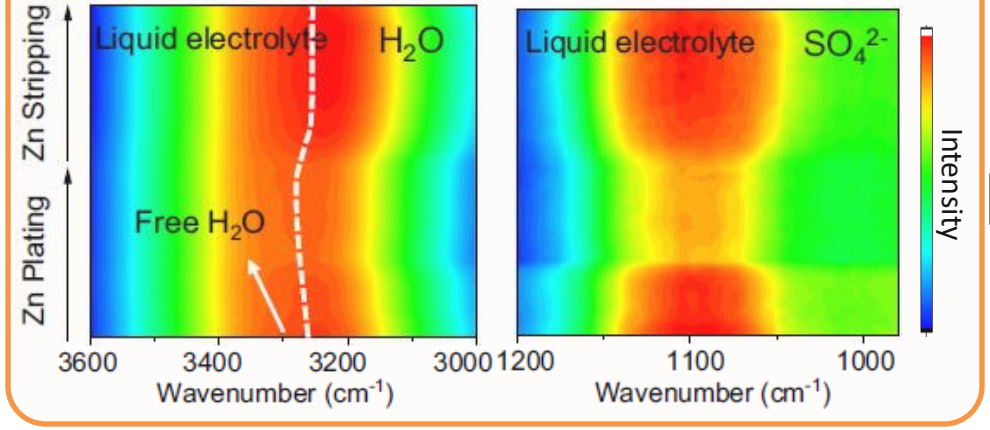

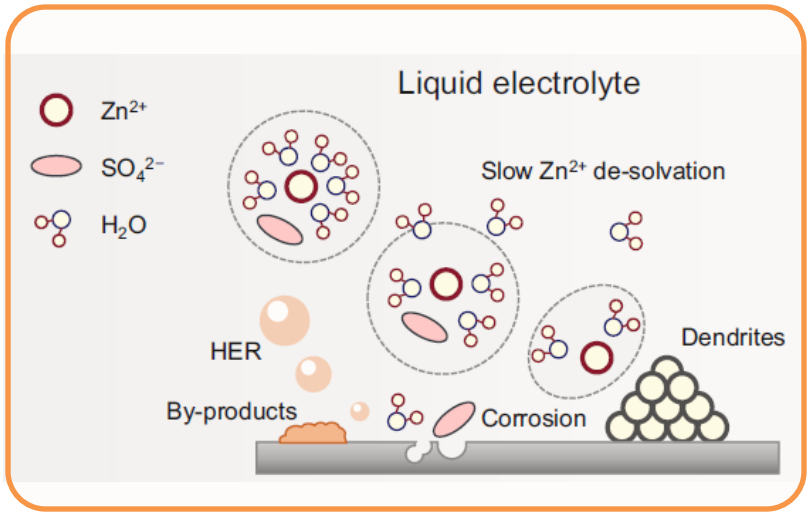

Ref: **G. Li**, Z. Zhao, S. Zhang, L. Sun, M. Li, J. A. Yuwono, J. Mao, J. Hao, **J. Vongsvivut**, L. Xing, C.-X. Zhao, Z. Guo, "A Biocompatible Electrolyte Enables Highly Reversible Zn Anode for Zinc Ion Battery," *Nat. Comm.* (2023), **14**, *1*, 6526.

ACKNOWLEDGEMENTS

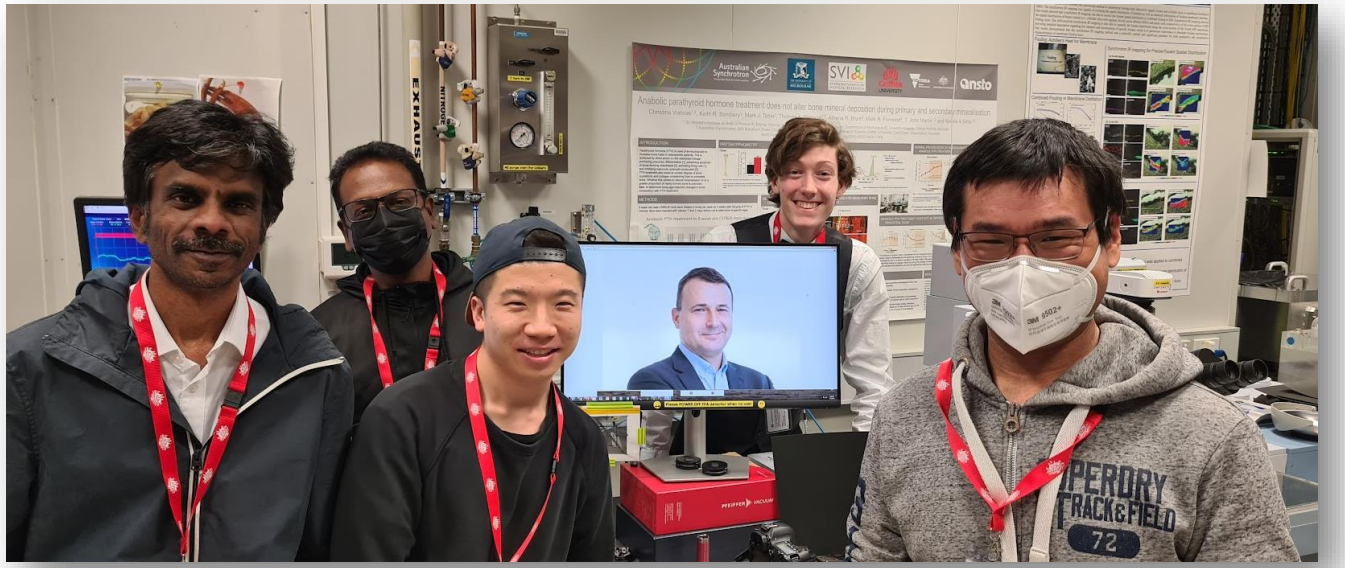

Monash Science Centre For Biospectroscopy

Callum Gassner
Bayden R. Wood

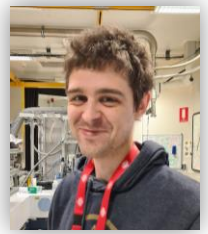

RMIT UNIVERSITY

Pooja Takkalkar
Nhol Kao
Gregory Griffin
Tapasi Mukherjee

SWINBURNE UNIVERSITY OF TECHNOLOGY

Nishar Hameed
Nisa V. Salim
Ahmed Al-Qatatsheh
Jaworski C. Capricho
Premika Govindaraj

SWINBURNE UNIVERSITY OF TECHNOLOGY

Saulius Juodkazis
Soon Hock Ng
Vijayakumar Anand
Molong Han
Daniel Smith
Armandas Balčytis

Tokyo Institute of Technology

Junko Morikawa
Meguya Ryu
Reo Honda

SVI ST VINCENT'S INSTITUTE MEDICAL RESEARCH

Natalie A. Sims
Martha A. Blank
Christina Vrahnas
Ingrid Poulton
Blessing Crimeen-Irwin

Australian Academy of Science

Financial support: Regional Collaborations Programme COVID-19 digital grant 2020
"Web platform for remote data analysis and processing of synchrotron data"

ACKNOWLEDGEMENTS

Monash Science Centre For Biospectroscopy

Don McNaughton
Bayden R. Wood
Philip Heraud
David Perez-Guita
Serena Ch'ng (AINSE-Honours)
Ben Boyd
Malinda Salim
Andrew Clulow

Institut Pasteur

Didier Menard
Eric Legrand

Tokyo Institute of Technology

Junko Morikawa
Meguya Ryu
Reo Honda

Curtin University

Simon Lewis
Wilhelm van Bronswjik
Mark J. Hackett
Georgiana Sauzier (AINSE-ECRA)
Elena Dallerba (AINSE-ECRA)
Ashley Hollings (AINSE-PGRA)
Rhiannon E. Boseley (AINSE-PGRA)
Karina Khambatta (AINSE-PGRA)
Keea Inder-Smith (AINSE-PGRA)
Meg Willans (AINSE-Honours)

THE UNIVERSITY OF MELBOURNE

Sally Gras
Lydia Ong
Anita Pax

4 AINSE Early Career Researcher Award (ECRA)

UNSW SYDNEY

Cordelia Selomulya
Yong Wang
Woojeong Kim

THE UNIVERSITY OF WESTERN AUSTRALIA

Ingrid Ward
Kane Ditchfield
Nikola Ristovski (AINSE-Honours)

UNIVERSITÄT BAYREUTH

Thomas Scheibel
Christian Haynl
Vanessa J. Neubauer
Kai R. H. Mayer

RMIT UNIVERSITY

Elena P. Ivanova
James Chapman
Vi Khanh Truong
Aaron Elbourne
Saffron Bryant
Zoe Shaw (AINSE-PGRA)
Louisa Huang (AINSE-PGRA)
Erim Kosyer (AINSE-Honours)
Soroosh Gharehgozlo (AINSE-Honours)
Nhol Kao
Gregory Griffin
Pooja Takkalkar
Benu Adhikari
Yakindra Timilsena

Flinders University

SWINBURNE UNIVERSITY OF TECHNOLOGY

Saulius Juodkazis
Armandas Balčytis
Soon Hock Ng
Nishar Hameed
Premika Govindaraj (PGRA)

DEAKIN UNIVERSITY AUSTRALIA Worldly

Lingxue Kong
Ludo Dumee
Jingshi Wang (AINSE-PGRA)
Srinivas Nunna

THE UNIVERSITY of ADELAIDE

Zaiping Guo
Wei Kong Pang
Sailin Liu (AINSE-PGRA/ECRA)
Shilin Zhang
Ruizhi Zhang
Guanjie Li

UNIVERSITY OF WOLLONGONG AUSTRALIA

IRM BeamTeam: past & current

Mark J. Tobin
Previous Principal Scientist
(IRM & THz)

Alan Easdon
Senior Mechanical
Technician

Pimm Vongsvivut
Senior Scientist – IRM

Keith Bambery
Senior Scientist – IRM

Annaleise Klein
Scientist – IRM

LinkedIn

Australian Government

ANSTO


THANK YOU ☺
NATIONAL
CENTRE FOR
SYNCHROTRON
SCIENCE